AD-A171 434 COMPUTATIONAL FLUID DYNAMIC STUDIES OF CERTAIN DUCTED BLUFF-BODY FLOWFIEL..(U) DAYTON UNIV OH RESEARCH INST M S RAJU ET AL. JUL 86 UDR-TR-85-82 1/1

UNCLASSIFIED AFWAL-TR-86-2004-VOL-1 F22615-84-C-2411 F/G 21/2 NL

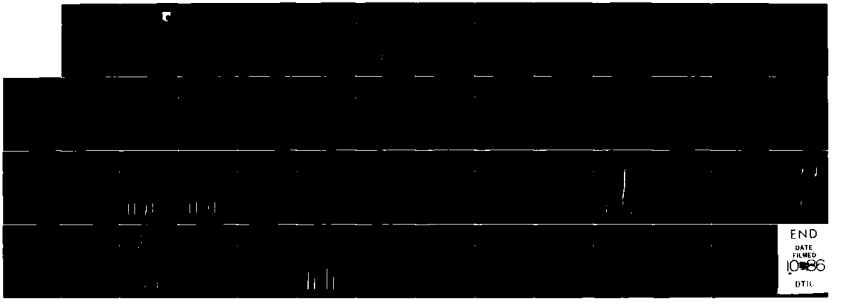

END

DATE FILMED

10-86

DTIC

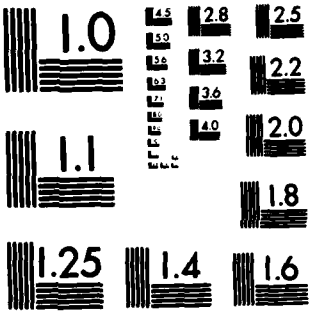

(2)

AFWAL-TR-86-2004
Volume I

COMPUTATIONAL FLUID DYNAMIC STUDIES OF CERTAIN DUCTED BLUFF-BODY FLOWFIELDS RELEVANT TO TURBOJET COMBUSTORS

VOLUME I - Time-Dependent Calculations with the k-ε Turbulence Model for an Existing Centerbody Combustor

M. S. Raju and L. Krishnamurthy
University of Dayton
Research Institute
Dayton, Ohio 45469-0001

July 1986

FINAL REPORT FOR PERIOD 16 AUGUST 1984 - 30 SEPTEMBER 1985

Approved for Public Release, Distribution Unlimited

AERO PROPULSION LABORATORY
AIR FORCE WRIGHT AERONAUTICAL LABORATORIES
AIR FORCE SYSTEMS COMMAND
WRIGHT-PATTERSON AIR FORCE BASE, OH 45433-6563

NOTICE

"When Government drawings, specifications, or other data are used for any purpose other than in connection with a definitely related government procurement operation, the United States Government thereby incurs no responsibility nor any obligation whatsoever; and the fact that the Government may have formulated, furnished, or in any other way supplied the said drawings, specifications, or other data, is not to be regarded by implication or otherwise as in any manner licensing the holder or any other person or corporation, or conveying any rights or permission to manufacture, use or sell any patented invention that may in any way be related thereto."

This report has been reviewed by the Office of Public Affairs (ASD/PA) and is releasable to the National Technical Information Service (NTIS). At NTIS, it will be available to the general public, including foreign nations.

This technical report has been reviewed and is approved for publication.

W. M. Roquemore

W.M. ROQUEMORE
Fuels Branch
Fuels and Lubrication Division
Aero Propulsion Laboratory

Arthur V. Churchill

ARTHUR V. CHURCHILL,
Chief, Fuels Branch
Fuels and Lubrication Division
Aero Propulsion Laboratory

FOR THE COMMANDER

Robert D. Sherrill

ROBERT D. SHERRILL, Chief
Fuels and Lubrication Division
Aero Propulsion Laboratory

"If your address has changed, if you wish to be removed from our mailing list, or if the addressee is no longer employed by your organization, please notify AFWAL/POSF, W-PAFB, OH 45433-6563 to help us maintain a current mailing list.

Copies of this report should not be returned unless return is required by security considerations, contractual obligations, or notice of a specific document.

Unclassified
SECURITY CLASSIFICATION OF THIS PAGE

AD-A171434

REPORT DOCUMENTATION PAGE

1a. REPORT SECURITY CLASSIFICATION: Unclassified	1b. RESTRICTIVE MARKINGS: N/A
2a. SECURITY CLASSIFICATION AUTHORITY: N/A	3. DISTRIBUTION/AVAILABILITY OF REPORT: Approved for Public Release, Distribution Unlimited
2b. DECLASSIFICATION/DOWNGRADING SCHEDULE: N/A	
4. PERFORMING ORGANIZATION REPORT NUMBER(S): UDR-TR-85-82	5. MONITORING ORGANIZATION REPORT NUMBER(S): AFWAL-TR-86-2004, Volume I
6a. NAME OF PERFORMING ORGANIZATION: University of Dayton Research Institute; 6b. OFFICE SYMBOL (If applicable):	7a. NAME OF MONITORING ORGANIZATION: Aero Propulsion Laboratory (AFSC) Air Force Wright Aeronautical Laboratory
6c. ADDRESS (City, State and ZIP Code): Dayton, OH 45469-0001	7b. ADDRESS (City, State and ZIP Code): AFWAL/POSF Wright-Patterson Air Force Base, OH 45433-6563
8a. NAME OF FUNDING/SPONSORING ORGANIZATION; 8b. OFFICE SYMBOL (If applicable): AFWAL/POSF	9. PROCUREMENT INSTRUMENT IDENTIFICATION NUMBER: F33615-84-C-2411, Task 02
8c. ADDRESS (City, State and ZIP Code):	10. SOURCE OF FUNDING NOS.

PROGRAM ELEMENT NO.	PROJECT NO.	TASK NO.	WORK UNIT NO.
62203F	3048	05	43

11. TITLE (Include Security Classification): (See Reverse Side)

12. PERSONAL AUTHOR(S): M. S. Raju and L. Krishnamurthy

13a. TYPE OF REPORT	13b. TIME COVERED	14. DATE OF REPORT (Yr., Mo., Day)	15. PAGE COUNT
Final Report	FROM 8/16/84 TO 9/30/85	July 1986	46

16. SUPPLEMENTARY NOTATION: Work performed under the Scholarly Research Program

17. COSATI CODES		
FIELD	GROUP	SUB. GR.
2102	2104	2105

18. SUBJECT TERMS (Continue on reverse if necessary and identify by block number): Bluff-Body Near Wake; Confined Turbulent Flows; Nonreacting Flows; Recirculating Flows (See Reverse Side)

19. ABSTRACT (Continue on reverse if necessary and identify by block number)

A numerical investigation of the near-wake region in a ducted bluff-body combustor by finite-difference computations is reported. The numerical predictions are based upon the time-dependent, compressible Navier-Stokes equations and the k-ε turbulence model. The standard k-ε turbulence model ~~has been~~ modified to account for the nonstationary terms. The time-dependent calculations ~~have~~ addressed the nonreacting near-wake flowfield of the centerbody combustor with only the annular air stream present.

Flowfield predictions for a combustor inlet mass flow of 2 kg/s with the time-dependent formulation incorporating the k-ε turbulence model show the attainment of a steady-state recirculating flow in the near wake. The slow axial migration of the recirculation vortex towards the exit boundary which was noticed in the earlier time-dependent calculations without a turbulence model is no longer present. ~~Thus, the~~ present results have eliminated the appearance of reverse flow. (See Reverse Side)

20. DISTRIBUTION/AVAILABILITY OF ABSTRACT	21. ABSTRACT SECURITY CLASSIFICATION
UNCLASSIFIED/UNLIMITED ☒ SAME AS RPT. ☐ DTIC USERS ☐	Unclassified

22a. NAME OF RESPONSIBLE INDIVIDUAL	22b. TELEPHONE NUMBER (Include Area Code)	22c. OFFICE SYMBOL
W. M. Roquemore	(513) 255-6813	AFWAL/POSF

DD FORM 1473, 83 APR — EDITION OF 1 JAN 73 IS OBSOLETE.

Unclassified
SECURITY CLASSIFICATION OF THIS PAGE

BLOCK 11 (Continued)

Computational Fluid Dynamic Studies of Certain Ducted Bluff-Body Flowfields Relevant to Turbojet Combustors (U)

Volume I
Time-Dependent Calculations with the k-ε Turbulence Model for an Existing Centerbody Combustor

BLOCK 18 (Continued)

Unsteady Flow
Vortex Shedding

BLOCK 19 (Continued)

at the exit boundary with the consequent incompatibility of the boundary conditions, and thereby the spurious shedding-like behavior observed previously. The steady-state results in the present study demonstrate internal consistency with the time-averaged measurements and predictions for the locations of the vortex center and the centerline rear stagnation point. Preliminary computations for both laminar-like and turbulent flows with time-dependent perturbations of inflow boundary conditions do not show any oscillatory behavior in the interior of the combustor.

Present time-dependent turbulent computations with the MacCormack algorithm confirm the earlier observations (from the laminar-like calculations) of the inability of this computational procedure to accurately capture the dynamic features of the ducted centerbody combustor flowfields. It is likely that the experimental observations of the dynamic behavior of this configuration in reacting flows may have arisen from significant coupling between the duct acoustics and combustion heat release.

PREFACE

This final report was submitted by the University of Dayton, under Contract No. F33615-84-C-2411, Task 02. The research task, entitled "Assessment of Time-Dependent Calculations for Gas Turbine Combustor-Type Flows," was sponsored by the Scholarly Research Program of the Air Force Wright Aeronautical Laboratories, Aero Propulsion Laboratory, Wright-Patterson Air Force Base, Ohio, under Project No. 3048, Task 05, Work Unit 43. Dr. William M. Roquemore, AFWAL/POSF, was Project Engineer. The research work dealing with the time-dependent calculations reported in Volume I was initiated in August 1984 and completed in February 1985. The work describing the time-averaged calculations reported in Volume II was initiated, under an Extension of Task 02, in April 1985 and completed in August 1985. The numerical calculations were performed by Dr. M. S. Raju, Associate Research Engineer, and the report was written by Dr. L. Krishnamurthy, Senior Research Engineer. The authors express their appreciation to Dr. Roquemore for his interest and to Mr. J. S. Stutrud, AFWAL/POSF, for his help with their MODCOMP computer in the time-averaged calculations. The time-dependent computations were carried out on the CRAY-1S computer at the NASA Lewis Research Center and the authors express their appreciation to Dr. E. J. Mularz and Mr. R. W. Claus for their support of this computing activity. The authors also acknowledge the assistance of Ms. Ellen Bordewisch, Ms. Teresa Harding, and Ms. Marlene Haas, UDRI, in preparing this report, and Ms. Anita Cochran, UDRI in technical editing thereof.

TABLE OF CONTENTS

LIST OF ILLUSTRATIONS

SECTION I
INTRODUCTION

This final report (in two volumes) documents the results of the computational fluid dynamic (CFD) research performed by the University of Dayton for the Air Force Wright Aeronautical Laboratories, Aero Propulsion Laboratory (AFWAL/PO). The focus of this CFD research is the confined, turbulent recirculating flowfield behind a bluff body in the AFWAL/POSF research combustor.

In an existing version of the POSF combustor, a centerbody configuration, involving the turbulent mixing and combustion of an annular air stream and a central fuel jet in the near wake region of an axisymmetric bluff body, has been the subject of extensive diagnostic and predictive research. Computations of this configuration for the nonreacting flow due to the annular air alone have been performed with the time-dependent Navier-Stokes equations, incorporating a realistic turbulence model, and these results are presented here, in Volume I of this report. The time-averaged predictions based upon a solution of the Reynolds-Averaged Navier-Stokes equations for a proposed POSF combustor configuration, involving two annular air streams--a swirl-free outer stream and a swirling inner stream, a central fuel jet, and a centerbody imbedding the swirler and the fuel nozzle, are reported in Volume II.

1. BACKGROUND

The performance of a gas turbine is significantly influenced by the fluid mechanical and combustion processes in the combustion chamber. The details of the fluid motion and associated turbulence largely determine the mixing, combustion, and heat transfer characteristics of the combustor. Thus, an accurate prediction of turbulent mixing and combustion would require the knowledge of turbulence structure and turbulence

scales of a combustor flowfield. The viewpoint adopted for the prediction of turbulent flows is that they are the unsteady solutions of the Navier-Stokes equations[1] and that their description involves probabilistic features. Such a viewpoint, however, renders the prediction of turbulent reacting flows in realistic configurations like gas-turbine combustors exceedingly difficult, since the full unsteady nature of the flowfield must be computed even if one is interested only in its time-averaged behavior.

In principle, one can obtain the time-averaged information in two ways: either by solving the time-dependent Navier-Stokes equations and averaging the solutions, or by averaging these equations first and then solving them. In practice, however, both avenues suffer from major difficulties. Averaging the Navier-Stokes equations results in equations (whether they are the Reynolds-averaged equations in constant-density flows, or the Favre-averaged equations in variable-density flows) that are confronted by the indeterminacy known as the closure problem and by the consequent necessity to introduce a turbulence model. The direct and explicit computation of the time-dependent equations, on the other hand, has two drawbacks. First, a typical turbulent flowfield is characterized by a large number of interacting length scales, whose explicit computation by the numerical solution of the full equations at high Reynolds numbers requires enormous computing effort. The second source of difficulty is the apparent lack of uniqueness of the solutions: if any two realizations in time, with apparently identical initial and boundary conditions, are distinctly different, averaging makes sense only if all such realizations and their associated probabilities are known (Reference 1).

---

1 Although the fluid mechanical turbulence is generally accepted to be contained in and explained by the Navier-Stokes equations, they remain to be fully tested for completeness by computations.

2. IMPLICATIONS

The foregoing difficulties notwithstanding, CFD prediction of complex turbulent flows in practical systems has proceeded vigorously, based upon computations of the averaged equations. Indeed, such computations, involving the two-equation model (for the turbulent kinetic energy k and the rate of its dissipation ϵ), appear to provide reasonable predictions of the overall trends in gas turbine combustor-type flows and represent the accepted design tool in the industry (Reference 2). Nevertheless, we must recognize that these time-averaged computations are based upon relatively well-developed statistical approaches which assume the classical description of turbulence--a continuous cascading of large eddies into smaller dissipative scales with random interactions thereamong. Consequently, the quantitative predictions have acceptable accuracy only when we have the so-called "fully developed turbulence." Unfortunately, realistic turbulent flows of engineering importance do not become fully developed, and the predictive success therein requires the experimental calibration and optimization of the free parameters (arising from the closure of the equations).

An implication of greater significance for predictors is the existence of large-scale ("coherent") structures, which has received considerable attention recently from both turbulence and combustion researchers. Recent experiments (see, e.g., Reference 3) have led to the growing realization that the vorticity fluctuations in turbulence are not quite so random or incoherent as was previously supposed. This viewpoint suggests that turbulence should be computed as the creation, evolution, interaction, and decay of large-scale vortex structures. Although these organized structures and their interactions appear to play a dominant role in the transport of heat, mass, and momentum in combustor flowfields, the conventional averaging framework has not taken them into account. Indeed, the concept of quasi-ordered, large-scale structures remains a challenging

and hitherto unsolved problem for predictors, since these structures are neither deterministic nor stochastic.

3. PREVIOUS WORK

A direct computation of the large-scale structures by means of the time-dependent Navier-Stokes equations has become an increasingly viable alternative. The application of such an approach to the POSF centerbody combustor was the subject of the recently completed CFD research program (Reference 4) at the University of Dayton Research Institute (UDRI). This idea was especially desirable in view of the photographic evidence (Reference 5) from combusting flow in the POSF configuration for the existence of nearly axisymmetric, toroidal vortices propagating downstream of the centerbody. The CFD examination of the POSF configuration for nonreacting flow (with only the annular air stream present) involved the application of the computational procedure (Reference 6) developed at AFWAL's Flight Dynamics Laboratory (FIMM).

The preliminary results (Reference 7) of the time-dependent computations and a computer-generated flowfield movie obtained therefrom appeared to demonstrate the ability of the FIMM procedure to simulate the processes of formation, growth, coalescence, and decay of the wake-vortex train. A comprehensive investigation (Reference 8), however, of the type as well as the parametric variation of the boundary conditions at the inlet, exit, and solid wall (both the centerbody and duct walls) failed to establish the previously seen (Reference 7) features of vortex shedding in the near wake. The computations with the time-dependent equations resulted in either a stationary vortex [reminiscent of the result (e.g., Reference 9) obtained with the time-averaged equations], or a numerically unstable unsteady flow. This demonstrated lack of a numerically stable unsteady flow from the time-dependent calculations was of major concern, in view of (a) the inherently unsteady nature of the separated

shear layer and of the recirculating flow in a bluff-body wake in general and (b) the experimental evidence from the POSF configuration in particular.

An assessment of the time-dependent calculations (Reference 8) emphasized that the shedding-like behavior observed in Reference 7 may be neither self-sustaining nor physical and that a conclusive demonstration of the successful simulation of the dynamic features of subsonic internal flows was still unavailable. A posteriori reflection indicates that such an assessment should not be surprising.

A turbulent flowfield (such as that in the POSF combustor) is characterized by a large number of randomly interacting length scales which range from scales as large as a typical macroscopic dimension (e.g., the centerbody diameter) to ones as small as the Kolmogorov dissipative scales. A computational grid resolving the smallest scales would require grid points N on the order of $Re^{9/4}$ (Reference 10), where Re is the representative local Reynolds number. Estimated values of N for realistic flowfields are extremely large, on the order of 10^{13} and higher (Reference 11). Thus, the direct computation at high Reynolds numbers with the full three-dimensional, time-dependent equations entails enormous computing effort. Indeed, with the present-day computers and even those of the foreseeable future, the explicitly resolved smallest scale is very much larger than the dissipation scale, and accurate solutions of the full equations can be computed only at very low Reynolds numbers.

Current approach to direct time-dependent computation, therefore, can be only a "large-eddy simulation" (LES) at best, wherein the full three-dimensional equations are solved only for scales larger than a selected cutoff length. An accurate LES then clearly requires a "subgrid-scale" turbulence closure model to account for the smaller scales below the LES cutoff length. While the selected cutoff between large and small scales is

arbitrary and a function of the available computing power, and the fraction of the spectrum of energy containing turbulent motions that can be explicitly computed will grow toward unity as machines become larger and faster, this technology-imposed cutoff is unlikely to approach the order of the Kolmogorov scale in high-Reynolds-number flows.

The time-dependent computations of the previous study (Reference 4) are not truly representative of LES. A minor drawback of the original FIMM procedure (Reference 6) was that the calculations were axisymmetric, whereas the large eddies are three-dimensional and anisotropic. A serious defect in the POSF combustor results obtained in Reference 7 and in subsequent investigations (Reference 8) was the absence of a turbulence model. While the FIMM procedure was essentially a Reynolds-averaged formulation [with the closure obtained at all scales through the Baldwin-Lomax model (Reference 12) of the mixing-length type], the previous POSF results were obtained from laminar-like calculations, since no eddy viscosity was employed. Although it is instructive to regard these calculations (in References 7,8) employing the molecular viscosity as a special subcase of the Reynolds-averaged simulation with zero turbulence, its relevance to the high-Reynolds-number flows under consideration is highly questionable. The argument that the numerical procedure does introduce an artificial viscosity is not entirely satisfying, since the extent to which the numerical artifact mimics physical turbulence is not known.

A more serious problem in the time-dependent computations may be due to the MacCormack algorithm. This algorithm was rejected by the Stanford University LES proponents, because of its propensity to be highly energy dissipative (Reference 13). Thus, the asymptotic tendency to a stationary vortex in the near wake observed in several of our POSF numerical experiments (Reference 8) may well have been caused by this apparent energy dissipation of numerical origin. This conjecture appears to be supported by

the analysis of Feiereisen, et al. (Reference 13) which reveals that when an initial flowfield containing all length scales is advanced in time, the smallest scales (i.e., the highest wavenumbers) will swiftly disappear through the highly dissipative action of the numerical algorithm. A comprehensive assessment of time-dependent calculations must address this aspect.

4. SCOPE OF PRESENT WORK

An assessment of time-dependent calculations for gas turbine combustor-type flows entails both unsteady- and steady-state computations. A comprehensive CFD research of unsteady modeling for the class of ducted, internal flows of high Reynolds number and low Mach number representative of gas turbine combustor-type configurations must involve a survey, selection, and review of potential computational schemes in the literature, and an evaluation of several time-dependent procedures of relevance through comparative calculations of appropriate configurations. The choice of these configurations must be governed by several factors such as geometric simplicity, ease of specification of boundary conditions that can be prescribed or measured, and availability of accurate time-averaged and time-resolved experimental data in both nonreacting and reacting flows. Potential candidates which can satisfy the requirements for the test configurations are likely to be few. Axisymmetric and planar mixing layers of the type investigated at the California Institute of Technology appear to be attractive possibilities. The dominant interest here, however, is concerned with the POSF research combustor, involving both centerbody and noncenterbody test sections. It is essential that the evaluation of the computational schemes must be based on their numerical accuracy and computational efficiency; their suitability for use in complex combusting geometries; their ability to be extended to include combustion, swirl, and three-dimensional flowfields; and their accuracy in comparison with experimental data. Of the

different computational procedures available, only the FIMM code (Reference 6) involving the MacCormack explicit algorithm has been previously examined (Reference 8) in detail for the POSF configuration. Despite the major uncertainties in the MacCormack procedure, alluded to in Paragraph I.3, this algorithm was expected to remain as a benchmark against which other computational procedures could be judged.

The limited scope of the Scholarly Research Program, however, meant a much less comprehensive CFD examination of the unsteady flow in the existing POSF centerbody combustor. Such a limited investigation, which is documented here, essentially involved an extension of our earlier studies (Reference 8) by properly incorporating the k-ϵ turbulence model of Jones and Launder (see References 14-16) into the FIMM (Reference 6) calculation procedure employed previously (References 7,8). The two additional equations for k and ϵ are solved in the spirit of MacCormack's algorithm involving a forward-predictor, backward-corrector sequence at each time step. These refined calculations with the time-dependent formulation show that the flowfield reaches a steady state asymptotically. Furthermore, the characteristics of the recirculation zone and the values of the flow variables obtained in these calculations closely correspond to the experimental observations. Present results further demonstrate that the time-dependent computations lacking a turbulence model for properly accounting for the dissipation that is inherently present at the high-Reynolds-number flows in configurations such as the POSF combustor will invariably lead to solutions (Reference 7) that are physically unrealistic at best.

The steady-state calculations were expected to involve a refined version (Reference 17) of the Reynolds-averaged formulation. Because of the improved physical and numerical modeling aspects of Reference 17, this steady-state procedure was anticipated to yield better predictions than the results obtained earlier (References 8,9). Of particular interest in this context

is the new POSF combustor configuration under consideration for development and testing. This baseline configuration involving the mixing of two annular air streams (an outer swirl-free stream and an inner swirling stream) and a central fuel jet in the near wake of a ducted bluff body is expected to simulate more realistically the primary zone of a gas-turbine combustor than did the earlier centerbody configuration. Time-averaged computational experiments prior to and during the actual POSF experiments could serve in guiding the selection of optimum conditions for further development. The time-averaged calculations of the proposed POSF combustor are discussed in Volume II.

5. OUTLINE OF REPORT

The incorporation of the k-ϵ model into the time-dependent formulation is presented in Section II. Section III reports the results of the time-dependent calculations and shows the influence of the explicit introduction of turbulence in these calculations. Also presented in this section are some results of laminar-like calculations but with forcing achieved through time-dependent inflow conditions. The conclusions and recommendations from this study are outlined in Section IV.

SECTION II
TIME-DEPENDENT FORMULATION

This section discusses the introduction of the two-equation turbulence model for the calculation of the nonreacting flow in the POSF centerbody combustor with the time-dependent Navier-Stokes equations. The adaptation of the FIMM computational procedure (Reference 6) is extensively discussed in Reference 8 and the reader is referred to that discussion for details.

1. GOVERNING EQUATIONS

As in the previous studies (References 7,8), the unsteady flowfield in the centerbody configuration is examined here only for the nonreacting situation arising from the presence of annular air stream alone. Thus, both the previous and present CFD research does not address the observed (Reference 5) dynamic behavior in the centerbody near wake which involved combustion of the central fuel jet with annular air stream.

The set of governing equations comprising the time-dependent, axisymmetric, compressible Navier-Stokes equations of a perfect gas and describing the conservation of mass, momentum, and energy may be written in conservative form in physical space as follows:

$$\frac{\partial E}{\partial t} + \frac{\partial F}{\partial t} + \frac{1}{r}\frac{\partial rG}{\partial r} = H. \qquad (1)$$

Here, the column vectors E, F, G, and H respectively represent the fluxes corresponding to the time-dependent terms, axial and radial convective terms, and the source terms. These are explicitly presented as:

$$E = \begin{bmatrix} \rho \\ \rho U \\ \rho V \\ \rho e \\ \rho k \\ \rho \epsilon \end{bmatrix}, \quad F = \begin{bmatrix} \rho U \\ \rho U^2 - \tau_{xx} \\ \rho UV - \tau_{rx} \\ \rho Ue - U\tau_{xx} - V\tau_{xr} - \kappa T_x \\ \rho Uk - (\mu/\sigma_k)k_x \\ \rho U\epsilon - (\mu/\sigma_\epsilon)\epsilon_x \end{bmatrix},$$

$$G = \begin{bmatrix} \rho V \\ \rho UV - \tau_{rx} \\ \rho V2 - \tau_{rr} \\ \rho Ve - V\tau_{rr} - U\tau_{xr} - \kappa T_r \\ \rho Vk - (\mu/\sigma_k)k_r \\ \rho V\epsilon - (\mu/\sigma_\epsilon)\epsilon_r \end{bmatrix} \text{ and } H = \begin{bmatrix} 0 \\ 0 \\ -\tau_{\theta\theta}/r \\ 0 \\ P_k - \rho\epsilon \\ C_1(\epsilon/k)P_k \\ \quad - C_2\rho\epsilon^2/k \end{bmatrix}. \tag{2}$$

In Equation (2) the subscripts x and r denote partial derivatives with respect to the axial and radial coordinates respectively; the normal and shear stresses are given by:

$$\tau_{xx} = (2\mu + \lambda)\frac{\partial U}{\partial x} + \lambda\left(\frac{V}{r} + \frac{\partial V}{\partial r}\right) - P$$

$$\tau_{rr} = (2\mu + \lambda)\frac{\partial V}{\partial r} + \lambda\left(\frac{V}{r} + \frac{\partial U}{\partial x}\right) - P \tag{3}$$

$$\tau_{\theta\theta} = (2\mu + \lambda)\frac{V}{r} + \lambda\left(\frac{\partial U}{\partial x} + \frac{\partial V}{\partial r}\right) - P$$

and

$$\tau_{xr} = \tau_{rx} = \mu\left(\frac{\partial U}{\partial r} + \frac{\partial V}{\partial x}\right);$$

the turbulent kinetic energy production term P_k represents the generation of turbulence energy by the interaction of mean velocity gradients and turbulent stresses and is given by:

$$P_k = \left[(2\mu_t + \lambda_t)\frac{\partial U}{\partial x} + \lambda_t\left(\frac{V}{r} + \frac{\partial V}{\partial r}\right)\right]\frac{\partial U}{\partial x} +$$

$$\left[(2\mu_t + \lambda_t)\frac{\partial V}{\partial r} + \lambda_t\left(\frac{V}{r} + \frac{\partial U}{\partial x}\right)\right]\frac{\partial V}{\partial r} + \qquad (4)$$

$$\left[(2\mu_t + \lambda_t)\frac{V}{r} + \lambda_t\left(\frac{\partial U}{\partial x} + \frac{\partial V}{\partial r}\right)\right]\frac{V}{r} + \mu_t\left(\frac{\partial U}{\partial r} + \frac{\partial V}{\partial x}\right)^2.$$

In Equations (2) through (4) μ is the effective viscosity given by:

$$\mu = \mu_\ell + \mu_t, \qquad (5)$$

where μ_ℓ is the molecular viscosity (which is specified according to Sutherland's law), and μ_t is the turbulent eddy viscosity. The latter is obtained from:

$$\mu_t = c_\mu \rho k^2/\varepsilon, \qquad (6)$$

where c_μ is usually taken to be a constant equal to 0·09. λ is the effective second viscosity coefficient and λ_t is the corresponding turbulent eddy coefficent. It is assumed that $\lambda = -(2/3)\mu$ and $\lambda_t = -(2/3)\mu_t$. κ is the effective coefficient of thermal conductivity given by:

$$\kappa = c_p(\mu_\ell/Pr_\ell + \mu_t/Pr_t), \qquad (7)$$

where the laminar and turbulent Prandtl numbers Pr_l and Pr_t are taken as 0·72 and 1 respectively, and c_p is the constant-pressure heat capacity. The remaining parameters and constants in the turbulence model are $\sigma_k = 1$, $\sigma_\epsilon = 1{\cdot}3$, $C_1 = 1{\cdot}44$ and $C_2 = 1{\cdot}92$.

It must be noted that except for the addition of the differential equations for k and ϵ and the corresponding expressions, parameters, and constants for the k-ϵ turbulence model, the set of governing equations is the same as the one used in the laminar-like calculations of References 7 and 8. It is assumed here that the turbulent gas motion is described by the two-parameter (k-ϵ) model of Jones and Launder (see References 14-16), but with the nonstationary terms taken into account. Additional discussion of the k-ϵ model and the refinements therein to account for the streamline curvature and the preferential influence of normal stresses in the dissipation equation (these effects were not considered for the present study) is available in References 8 and 9.

Finally, the pressure is related to temperature by the equation of state

$$p = \rho RT. \tag{8}$$

The governing differential equations are advanced in time by MacCormack's explicit and unsplit algorithm. The FIMM procedure of Shang (Reference 6) is further modified to solve for the additional equations for k and ϵ. These two equations are solved in the same spirit as MacCormack's algorithm involving a forward-predictor, backward-corrector sequence at each time step.

2. BOUNDARY AND INITIAL CONDITIONS

The boundary conditions for the inflow and outflow boundaries and at the solid wall are the following:

a. Inflow Boundary Conditions

ρ, ρU, ρV: Specified

$$\frac{\partial^2 T}{\partial x^2} = 0$$

$$k = 0.03U^2 \tag{9}$$

and

$$\epsilon = c_\mu k^{1.5}/\ell,$$

where $\ell = 0.03\,(R_d - R_c)$, R_d and R_c being the respective radii of the duct and centerbody.

b. Outflow Boundary Conditions

The boundary conditions for the exit boundary are as follows:

$$P = P_e$$

and

$$\frac{\partial \phi}{\partial x} = 0, \tag{10}$$

where ϕ = U, V, T, k and ϵ.

c. Solid-Wall Boundary Conditions

No-slip conditions (U = 0 and V = 0) are used along the duct and centerbody walls to specify the velocity components. The wall temperature is a specified constant. The wall pressure is calculated from the boundary-layer assumption that its normal derivative vanishes at the wall. The density is calculated from the equation of state. The two scalars of the turbulence model are given by k = 0 and $\partial\epsilon/\partial n = 0$ (where n is the direction normal to the wall).

The foregoing boundary conditions consist of the appropriate conditions for the laminar-like, time-dependent calculations of Reference 8 and those of k and ϵ equations for the Reynolds-averaged, time-independent calculations of References 8 and 9.

3. COMPUTATIONAL DETAILS

The computational grid employed for these calculations is the baseline domain consisting of 60 axial nodes and 46 radial nodes. Figure 1 shows this finite-difference grid which was used in the laminar-like calculations of Reference 7 and in some cases of similar calculations of Reference 8. Additional details of this grid are found in the latter. Note that exponential grid stretching is used to adequately resolve the flowfield in the anticipated regions of large gradients. Also, for the present low subsonic flows, an artificial viscosity (other than that inherent in the MacCormack scheme itself) is not needed due to the lack therein of the very strong flowfield gradients typically present in supersonic flows.

Although the emphasis of the present study was the explicit introduction of a realistic turbulence model into the time-dependent formulation and the resulting flowfield behavior of the POSF configuration, additional time-dependent calculations were made to examine the effect of external forcing. Both laminar-like and the turbulent situations were considered.

a. Laminar-Like Cases with Time-Dependent Inflow

These calculations used the extended (80 x 46) finite-difference grid of Reference 8. Three different cases were studied, with the combustor inlet mass flow being 2 kg/s for all of them. A sinusoidal time-dependent perturbation was imposed on one of the inflow boundary conditions, with the frequency being 128 Hz corresponding to the fundamental frequency in the

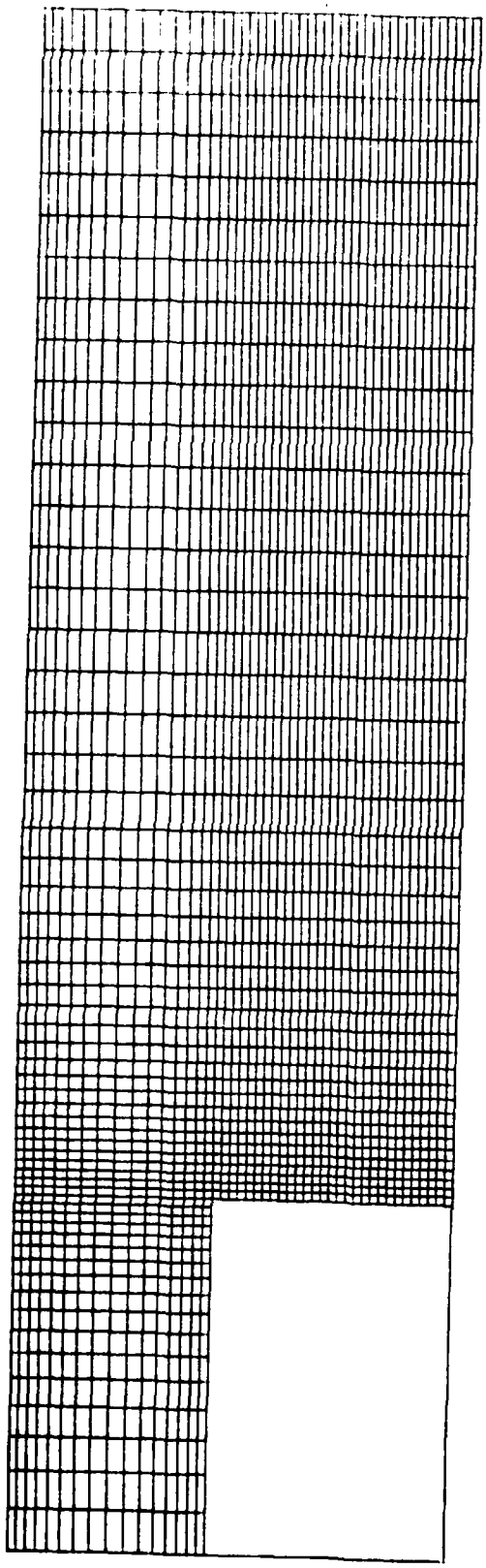

Figure 1. Baseline Finite - Difference Mesh (60 x 46).

mass-flow variations observed for the earlier computations (see p. 153 in Reference 8). The unperturbed parameters were akin to those of Case 7a in Reference 8.

(1) Case 1

The boundary conditions employed in this case are as follows:

(a) Inflow Conditions

$$\rho = 1{\cdot}1965 \text{ kg/m}^3$$

$$\rho U = \rho 48{\cdot}84 \ (1 + 0{\cdot}1 \sin ft)$$

$$\rho V = 0$$

$$\frac{\partial p}{\partial x} = 0$$

(b) Outflow Conditions

$$p = 9{,}821{\cdot}39 \text{ kg}_f/\text{m}^2, \quad r \leq R_c$$

$$\frac{\partial p}{\partial x} = 0, \qquad R_c < r \leq R_d$$

$$\frac{\partial U}{\partial x} = \frac{\partial V}{\partial x} = \frac{\partial T}{\partial x} = 0$$

(2) Case 2

The inflow and outflow conditions were the following:

(a) Inflow Conditions

$$\rho = 1{\cdot}1965 \text{ kg/m}^3$$

$$\rho U = \rho 48{\cdot}84[1 + 0{\cdot}1 \ (\sin ft + 0{\cdot}4 \sin 3ft)]$$

$$\rho V = 0$$

$$\frac{\partial p}{\partial x} = 0$$

(b) Outflow Conditions

$$p = 9{,}821{\cdot}39 \text{ kg}_f/\text{m}^2$$

$$\frac{\partial U}{\partial x} = \frac{\partial V}{\partial x} = \frac{\partial T}{\partial x} = 0$$

(3) Case 3

The following inflow and outflow conditions were employed:

(a) Inflow Conditions

$\rho = 1{\cdot}1965\ kg/m^3$

$\rho U = \rho 48{\cdot}84$

$\rho V = 0$

$p = p(2, J)\ (1 + 0{\cdot}1 \sin ft)$

(b) Outflow Conditions

$p = 9{,}821{\cdot}39\ kg_f/m^2$

$\frac{\partial U}{\partial x} = \frac{\partial V}{\partial x} = \frac{\partial T}{\partial x} = 0$

b. Turbulent Case with Time-Dependent Inflow

Only one case of time-dependent calculations with the k-ε model was considered with the forced inflow condition. The perturbation considered here is the same as that in Case 2 of the laminar-like calculations [see Paragraph II.3.a(2a)].

SECTION III
RESULTS AND DISCUSSION

This section presents the results of the time-dependent calculations with the k-ε turbulence model and those with the time-dependent inflow conditions for both laminar-like and turbulent cases. These numerical calculations were performed on the NASA Lewis Research Center CRAY-1S computer.

1. INFLUENCE OF TURBULENCE MODEL

Figure 2 shows the velocity-vector plots and vorticity-contour plots corresponding to the flowfield at 10,000, 20,000, 30,000, and 40,000 time steps. These results clearly show the attainment of a steady-state recirculating flow in the bluff-body near wake. It is interesting to note that even by the first 10,000 time steps, the initial transients have been washed off. Furthermore, recall our earlier observations in Reference 8 (e.g., Figures 58 and 59), according to which (a) the only unsteady flowfield feature was the slow axial propagation of the recirculation region toward the exit boundary (at an approximate speed of 3 m/s), and (b) the appearance of the reverse flow at this boundary triggered mass-flow oscillations. With the introduction of the k-ε turbulence model, this slow stretching and extension of the recirculation vortex appear to have been eliminated. Thus, continuation of the computations even up to 40,000 time steps does not encounter the downstream migration of the recirculating region, the approach of the reverse flow to the exit boundary, and the consequent incompatibility of the boundary conditions therein. These results, therefore, appear to substantiate our conjecture in Reference 8 that the lack of an adequate turbulence model might have caused the apparent unsteady behavior seen in References 7 and 8. Furthermore, the disappearance of the shedding-like behavior (observed earlier during the time period associated with the mass-flow fluctuations

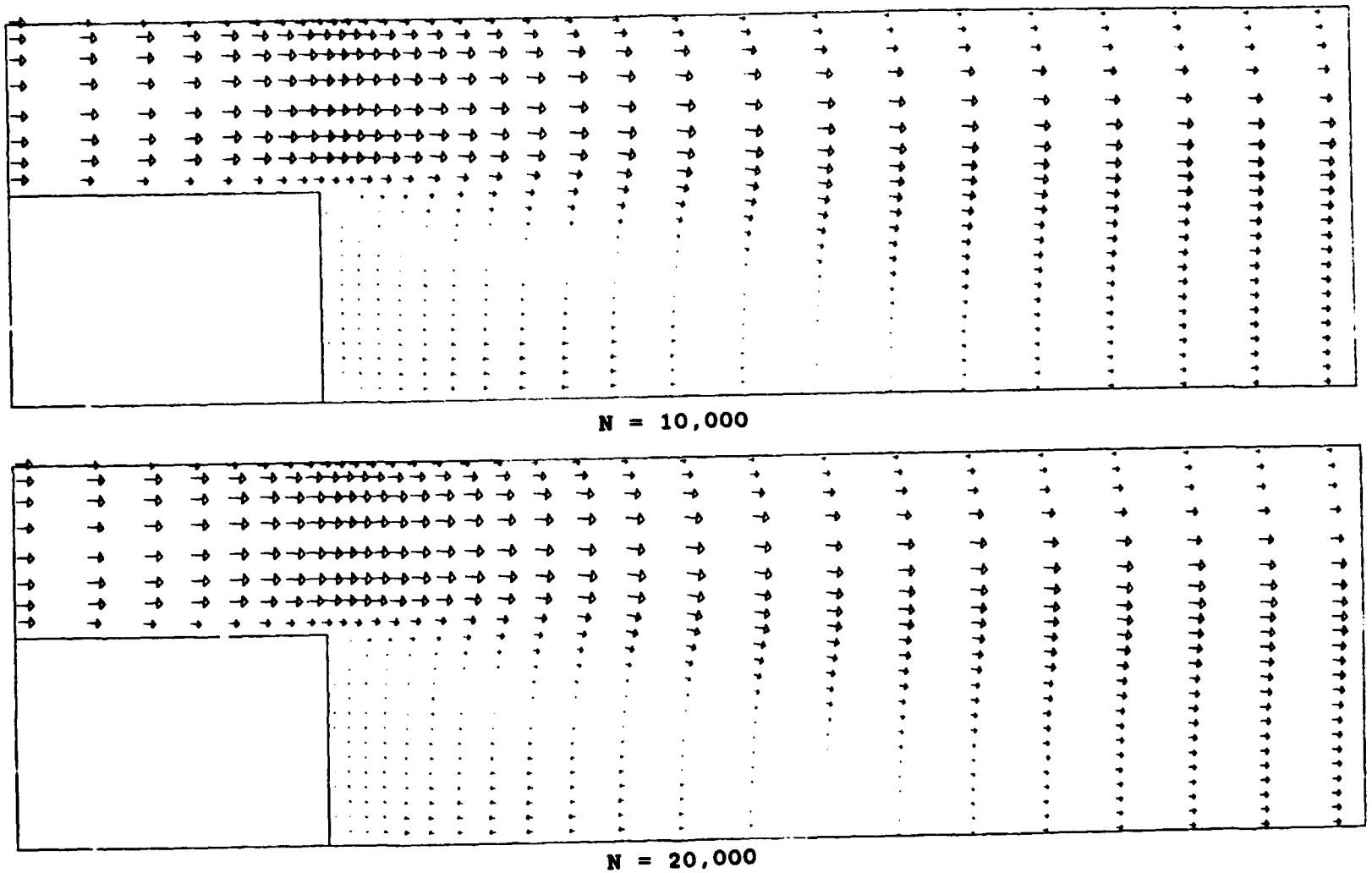

Figure 2(a). Velocity-Vector Plots for Turbulent Flow.

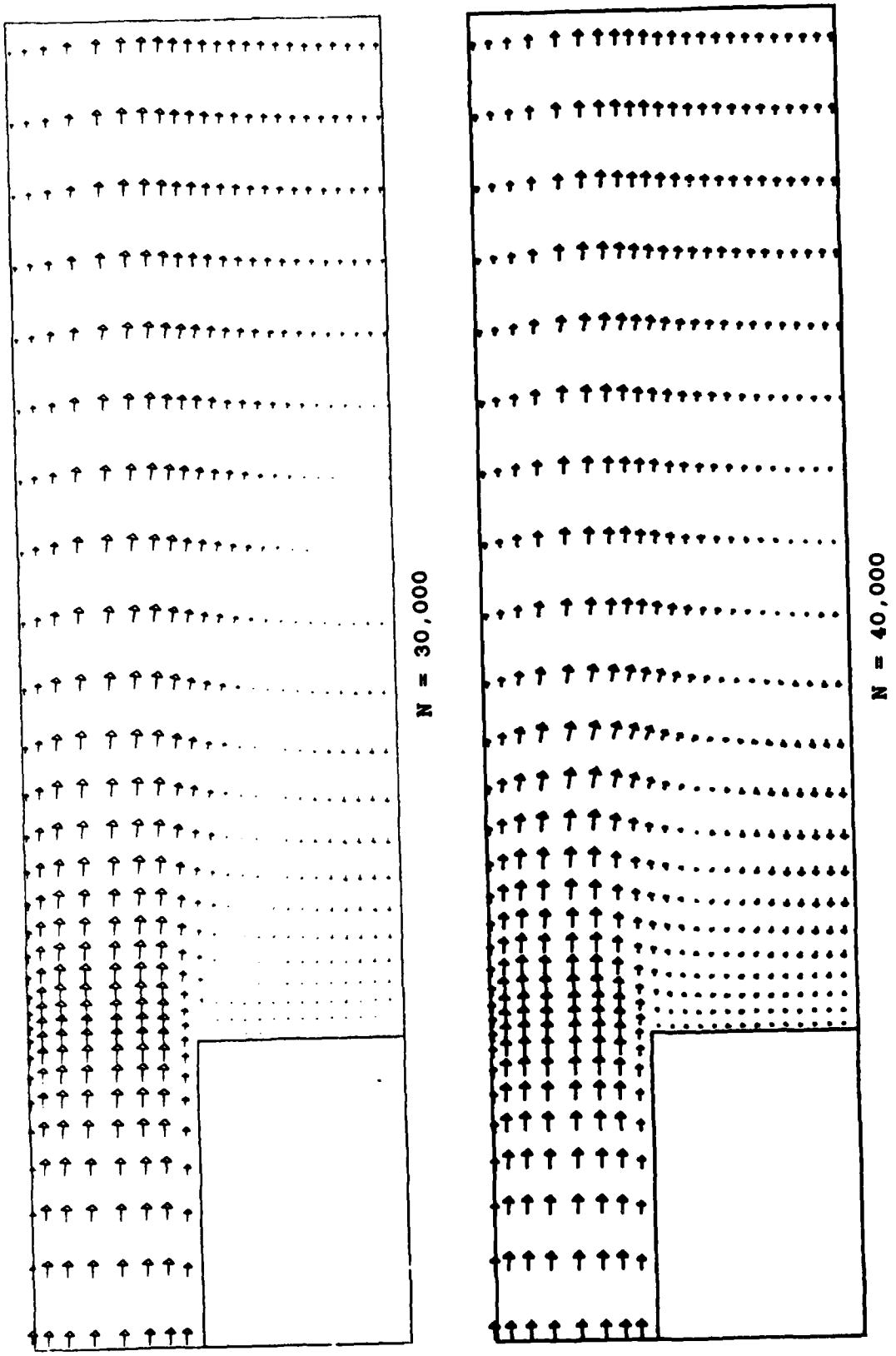

Figure 2(b). Velocity-Vector Plots for Turbulent Flow.

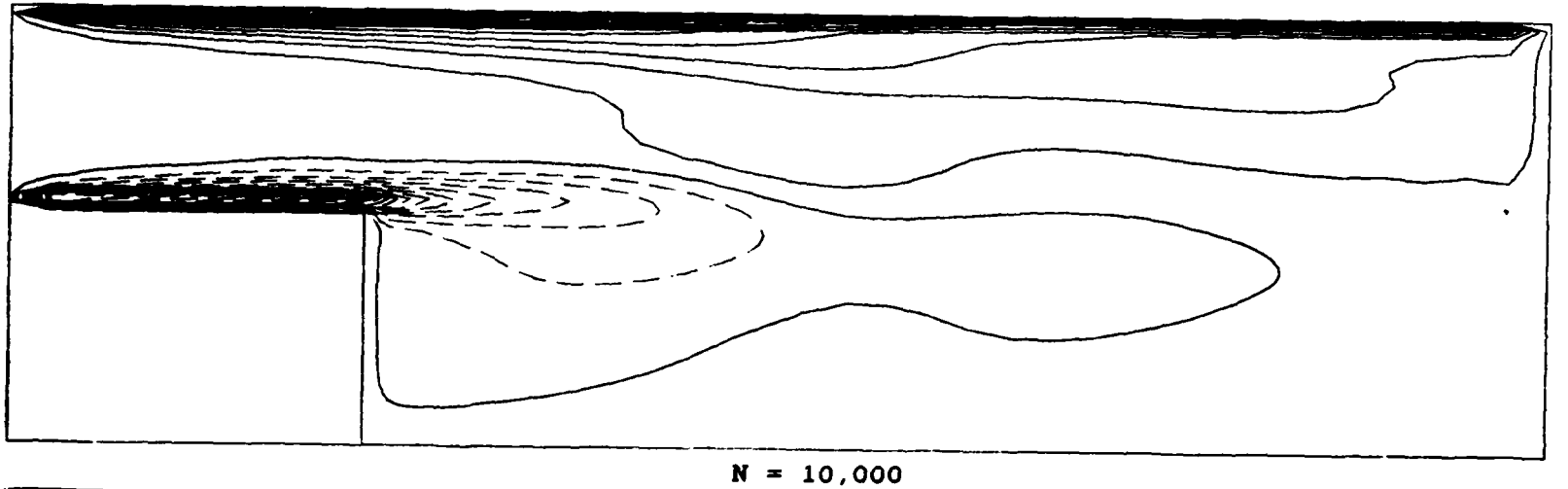

N = 10,000

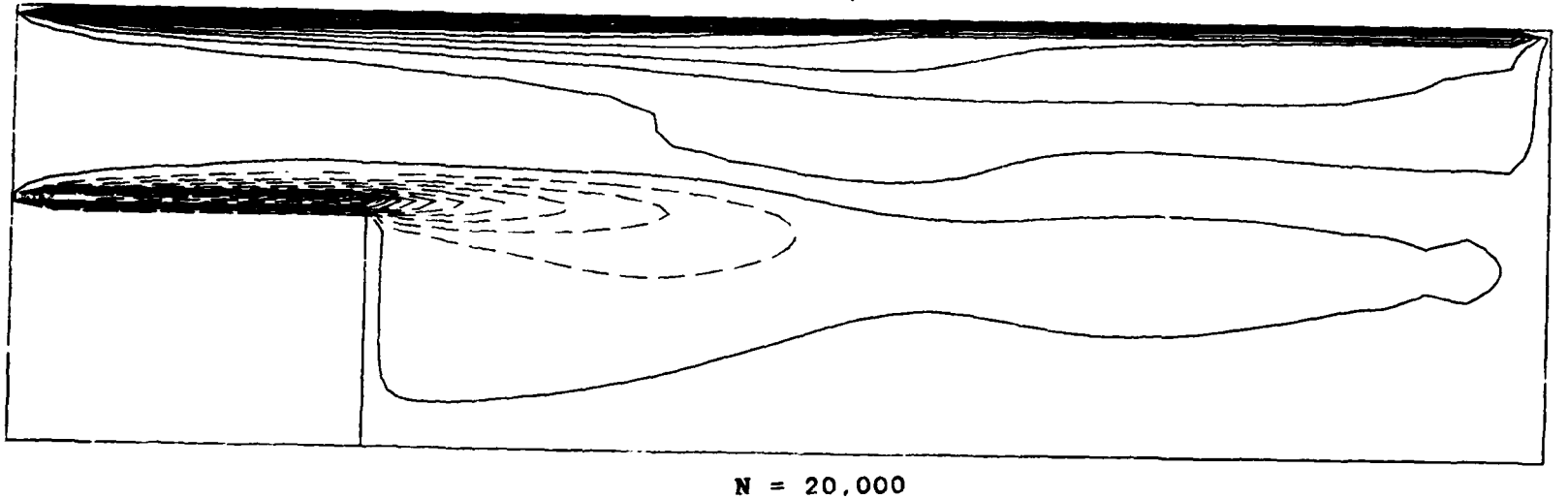

N = 20,000

Figure 2(c). Vorticity-Contour Plots for Turbulent Flow.

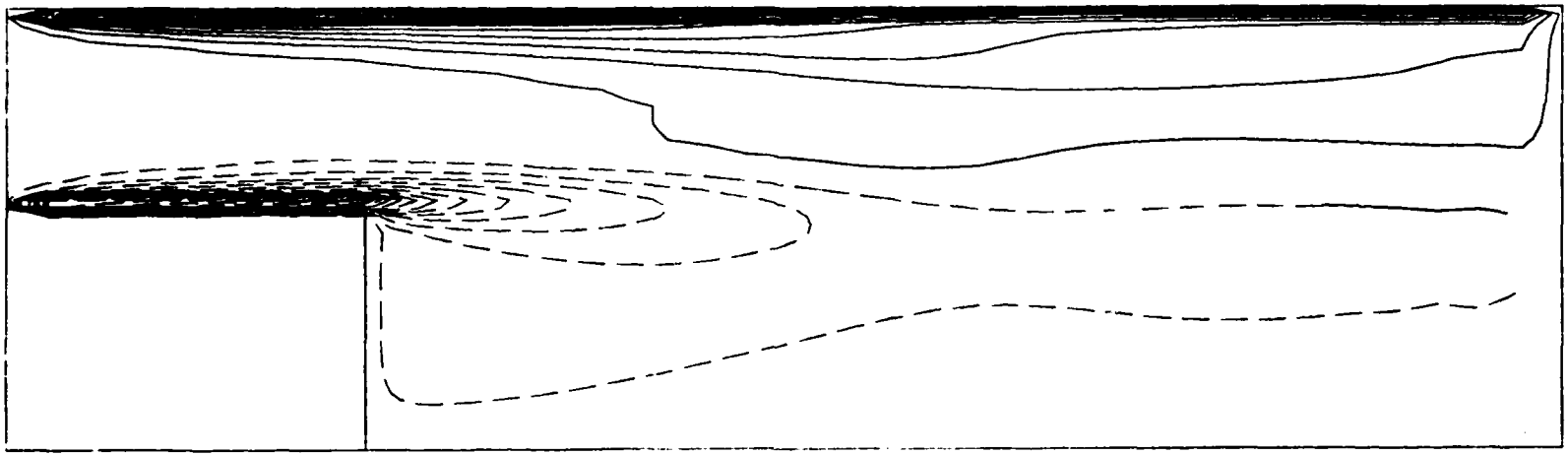

N = 30,000

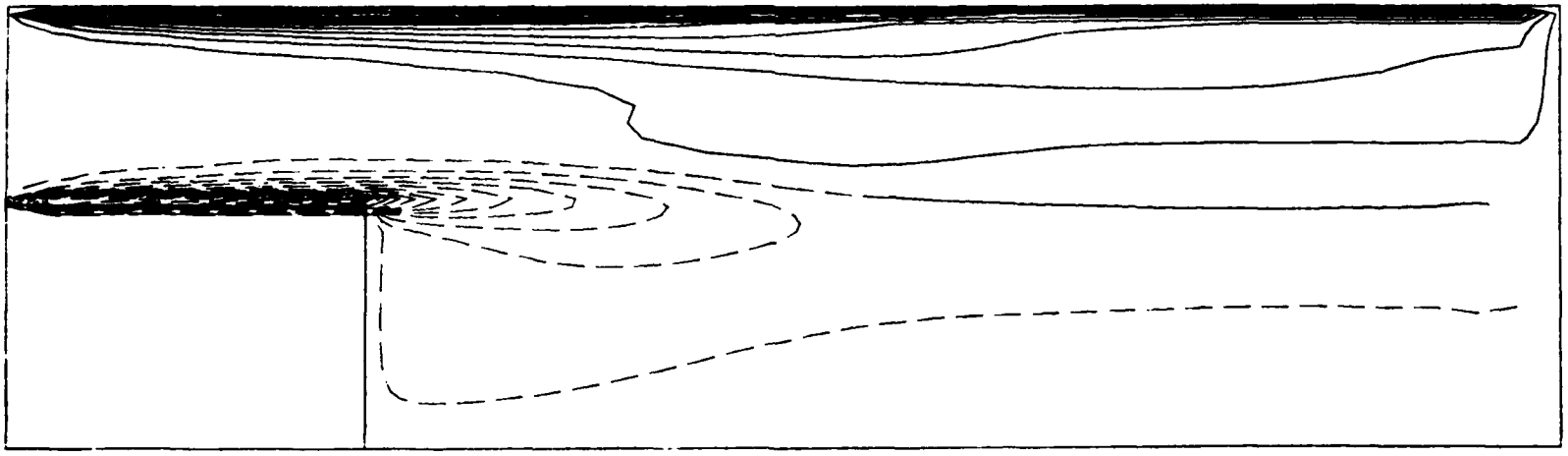

N = 40,000

Figure 2(d). Vorticty Contour Plots for Turbulent Flow.

triggered by the inadequacy of the outflow boundary conditions to handle the appearance of reverse flow there) resulting from the k-ϵ calculations lends credence to our claim that the dynamic behavior of the POSF combustor predicted in Reference 7 is neither self-sustaining nor physical, but is strictly a numerical artifact.

That the time-dependent solution of the POSF flowfield attains a steady state asymptotically after 40,000 time steps indicates a failure of the time-dependent formulation (subject to time-independent boundary and initial conditions) to yield a time-dependent flowfield in the interior. This, of course, is neither surprising nor undesirable, since the use of the time-dependent formulation to obtain the steady-state solution asymptotically for large times, when the physical problem does, in fact, possess a steady solution, is well known in CFD. Indeed, such an approach has been profitably exploited by Drummond (Reference 18) in his recent calculations of the turbulent reacting flow in a ramjet dump combustor. These calculations involved the unsplit MacCormack algorithm and a mixing-length type algebraic eddy viscosity model (Reference 19) to integrate the governing equations until a steady-state solution is reached. The calculated results were seen to indicate fair agreement overall with the experimental results for nonreacting flowfield. The observed overprediction of the rate of mixing of air and hydrogen streams is attributed in Reference 18 to the use of the simple algebraic turbulence model (Reference 19) which is not considered adequate to model the very complex turbulent flow of this configuration. The key point of interest to our present study is that the use of an even relatively crude mixing-length turbulence model in the time-dependent formulation has given rise to a steady-state solution which is consistent with experimental data.

This raises the interesting question as to how the steady-state solution from the time-dependent formulation compares with

the time-averaged solution and experimental data in the POSF configuration (References 8,9). A conclusive answer to this question requires an examination of the computed results of the velocity field (corresponding to the flowfield of Figure 2) for both the mean and rms quantities. Such an examination should address the axial (centerline) variation of the mean and rms axial velocity components (with the assumption of isotropy invoked necessarily for the latter), as well as the radial distribution at different axial stations of the axial and radial velocity components (for both mean and rms quantities). Such an examination was not within the scope of the present study.

An examination of the velocity-vector plots and the vorticity-contour plots of Figure 2, however, offers some clues. It is clearly seen that the centerline rear stagnation point in the velocity-vector plot occurs at a distance of approximately one centerbody diameter downstream of the centerbody. This result is consistent with both experimental results and time-averaged calculations (References 8,9). Another aspect demonstrating fair comparison relates to the vortex center of the large stationary vortex behind the centerbody. The axial and radial coordinates of the vortex center (where both the axial and radial mean velocity components vanish) in Figure 2d exhibit fair agreement with those obtained by the time-independent, Reynolds-averaged calculations (References 8 and 20). Note that while the calculations in Reference 8 were based upon an earlier version of the TEACH procedure (Reference 9), the results in Reference 20 were obtained from a more refined version (Reference 17) of the TEACH program. Thus, there is some evidence that the steady-state results obtained here from the time-dependent calculations with the k-ϵ model reasonably conform to the results of time-averaged measurements and calculations, thereby leading to an internal consistency between the time-averaged behavior and the steady-state behavior attained with the time-dependent formulation. This strongly suggests that a successful CFD

demonstration of the capability of the time-dependent formulation to predict in nonreacting POSF flowfield the dynamic features observed in combusting flow (Reference 5) remains to be carried out.

In this context, it is of interest to point out that the experimental observations (Reference 5) of the flame balls propagating downstream of the POSF centerbody, which revealed the presence of successive flame bursts and relative quiescence of a random nature, may arise from an altogether different mechanism. This mechanism is the coupling between combustion heat release and duct acoustics. Indeed, because of the nonlinear coupling between the governing equations for the conservation of momentum and energy, confined combustion is basically oscillatory. Such forced oscillations in combustion and their connection with the Rayleigh criterion which governs the coupling between the mechanical energy in the pressure wave and the thermal energy available from combustion heat release are well known in ramjets, turbojet afterburners, industrial furnaces, and rocket engines. If, in fact, the observed POSF dynamic features (Reference 5) are characteristic of a forced combustion system, the rationale (Reference 7) for seeking the dynamic behavior in nonreacting situations through a time-dependent formulation becomes suspect, since the essential coupling between duct acoustics and combustion heat release is missing in such a formulation. Here we recall the heuristic arguments presented by Reference 21 on the basis of time-averaged calculations and perturbations thereof to hint at the possibility of forced oscillations in the POSF combustor.

Conjectures on the behavior of the POSF configuration as representing a forced combustion system become more persuasive on different grounds as well. Available experimental and theoretical evidence (e.g., References 22-24) on the bluff-body flame stabilizers suggests that the flowfield structure during combustion and heat release exhibits drastic changes as compared

to an isothermal stream. The confined flowfield behind a two-dimensional bluff body has been observed (Reference 22) to become stationary at Reynolds numbers on the order of 10^4, due to the introduction of combustion, in contrast to the flowfield that is characterized by large-scale unsteady motion observed in nonreacting flowfields. Such a transition from a time-dependent flow to a time-independent flow caused by combustion has also been verified (Reference 23) by a Reynolds-averaged formulation (with the k-ϵ model) which retains explicit time dependence for the two-dimensional flow downstream of a ducted bluff body. Finally, the recent experiments (Reference 24) on the unconfined analog of the POSF centerbody configuration (albeit at small enough Reynolds numbers for the flow to be laminar) have also indicated the presence of vortex shedding from the bluff body in a nearly zero-heat-release, isothermal reacting flowfield (for a $TiCl_4$ - H_2O reaction), and the lack thereof in C_3H_8 - air combustion experiments.

The foregoing makes it clear that what is not open to doubt is the existence of the inherent unsteadiness of a separated shear layer downstream of the trailing blunt end of the centerbody and the initial appearance of the Kelvin-Helmholtz instability waves therefrom (note that very close to its origin where the displacement thickness is very small compared to the radius, this separated shear layer resembles the plane mixing layer downstream of a splitter plate and is extremely unstable to infinitesimal disturbances). What is beyond doubt is that in both axisymmetric and two-dimensional configurations, properly performed calculations of the time-dependent Navier-Stokes equations with a turbulence model (irrespective of its crudeness) do not capture the dynamic features but asymptotically lead to stationary states for large times. Therefore, the dynamic behavior shown in Reference 7 is not correct. This conclusion is further strengthened by our calculations with time-dependent inflow conditions.

2. EFFECT OF TIME-DEPENDENT INFLOW CONDITIONS

The results of time-dependent calculations to investigate the effect of external forcing are examined here, first for laminar-like cases (see Paragraph II.3.a), and then for one set of turbulent-flow calculations (see Paragraph II.3.b).

a. Laminar-Like Calculations

The velocity-vector plots and the vorticity-contour plots at different time steps for the three laminar cases [discussed in Paragraphs II.3.a(1) through (3)] are presented in Figures 3 through 5 respectively. As noted earlier, these calculations were completed for the extended domain and thus permit their proper comparison with the corresponding unforced computations of Reference 8. Present results show the initial shedding-like tendencies, the approach to a single recirculating vortex in the near wake, and its slow migration toward the exit boundary. The three different cases of forcing the inflow condition exhibit the same kind of flowfield behavior observed previously (Reference 8). There is no doubt that with the time-dependent inflow perturbations, there will be mass-flow fluctuations differing between the inlet and exit (these are not displayed here but they will be reminiscent of the behavior observed in Figures 58 and 59 of Reference 8). It is clear, however, that the overall flowfield does not exhibit a locked-on oscillatory behavior. It is conceivable that the amplitudes of the time-dependent perturbations are not sufficiently large for this lock-on to occur, even though the perturbing frequency corresponds to the fundamental frequency of the quarter-wave resonator for the longitudinal oscillations. There is a reason to suspect, however, that the temporal perturbations at the inflow boundary are damped out due to physical and/or numerical causes (recall the energy-dissipative tendency of the MacCormack

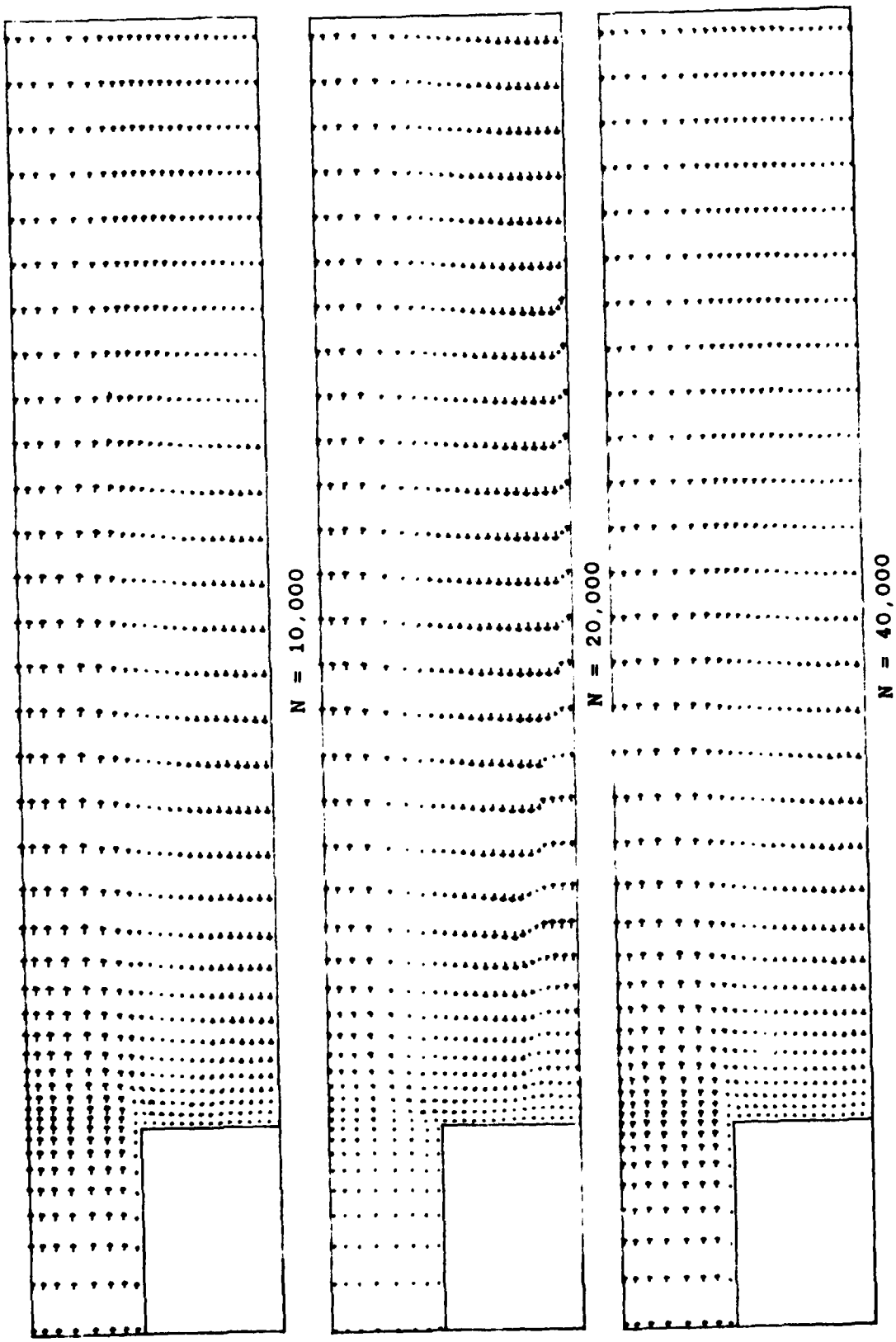

Figure 3(a). Velocity-Vector Plots for Laminar-Like Calculations (Case 1) with Forcing.

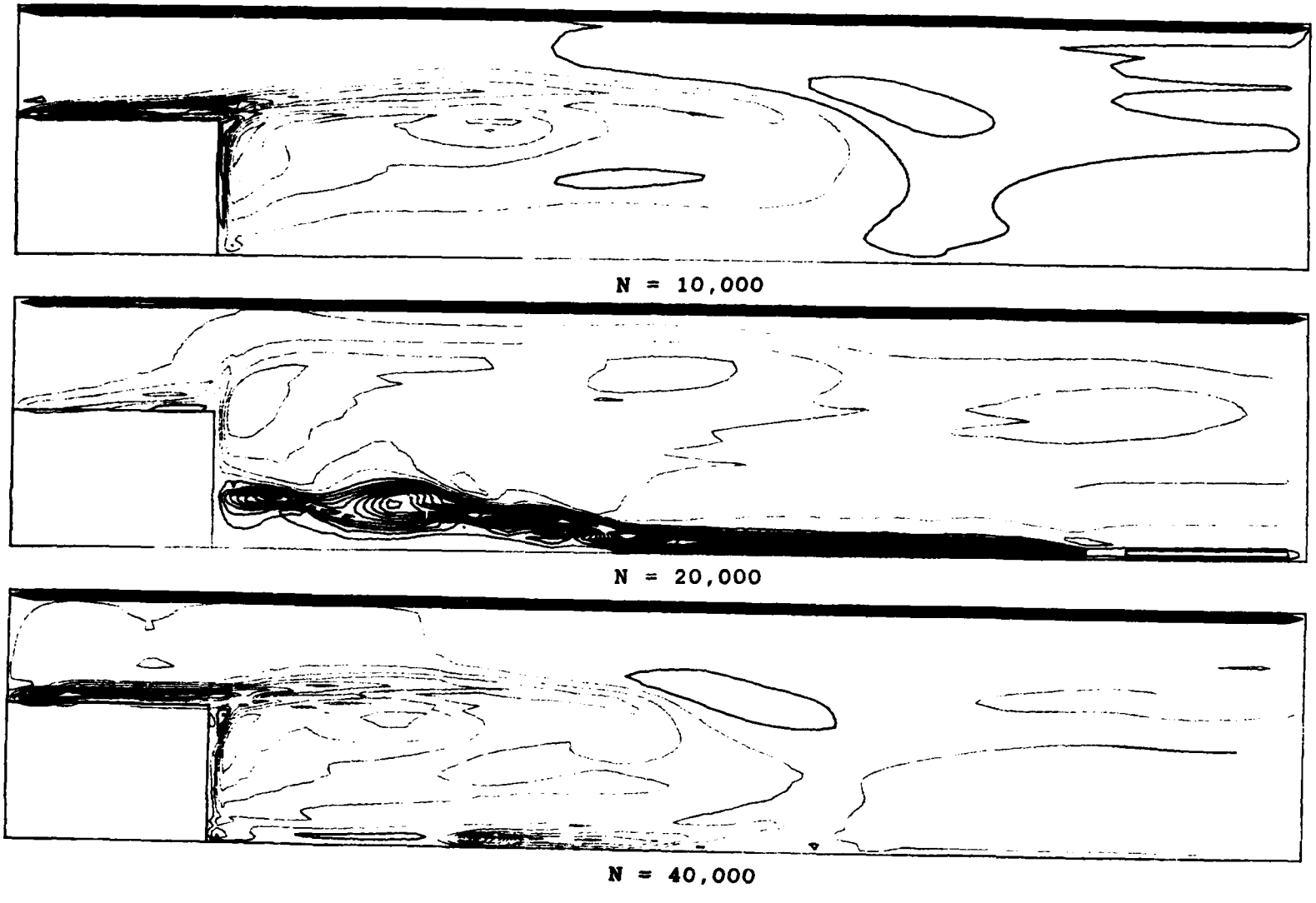

Figure 3(b). Vorticity-Contour Plots for Laminar-Like Calculations (Case 2) with Forcing.

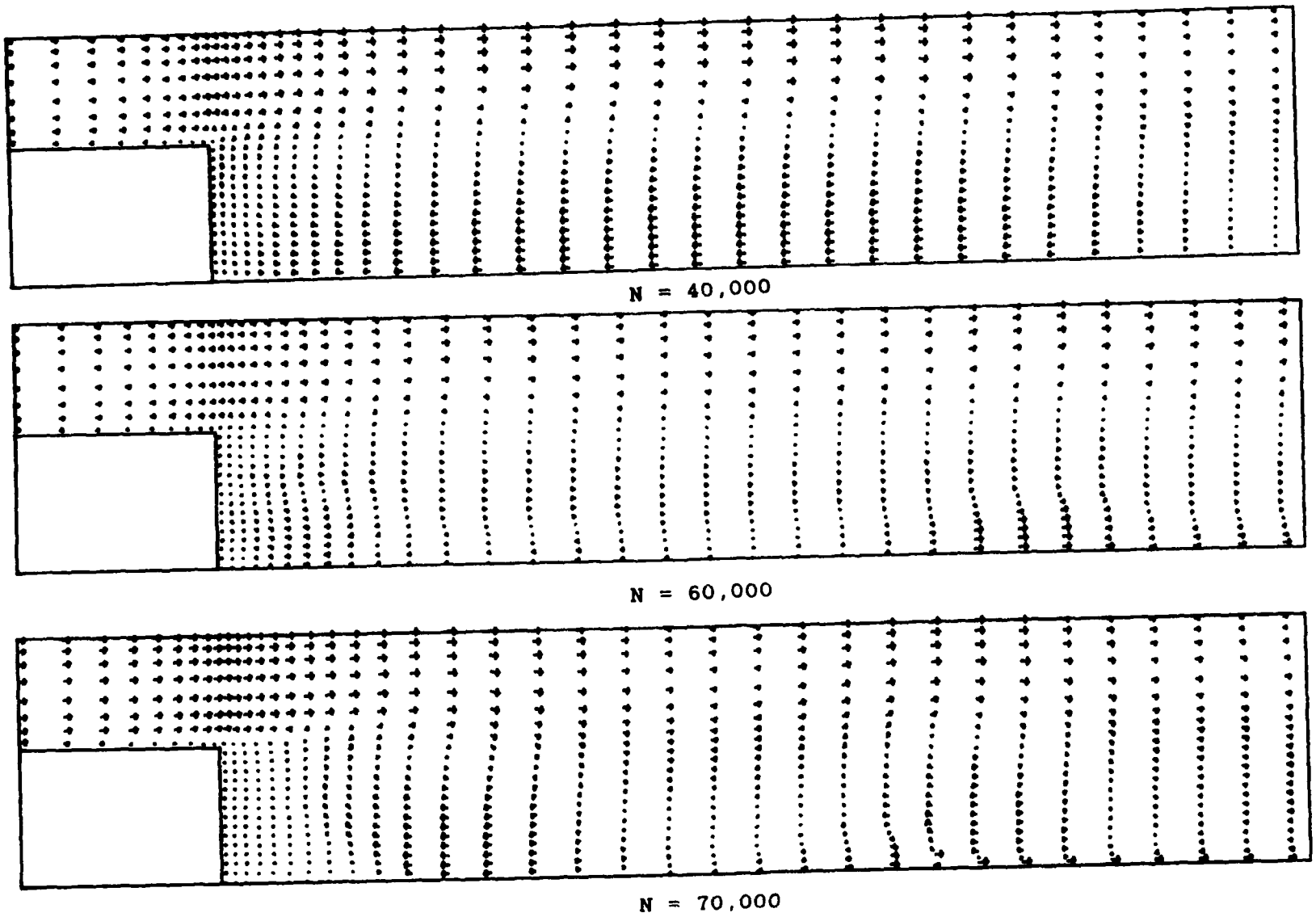

Figure 4(a). Velocity-Vector Plots for Laminar-Like Calculations (Case 2) with Forcing.

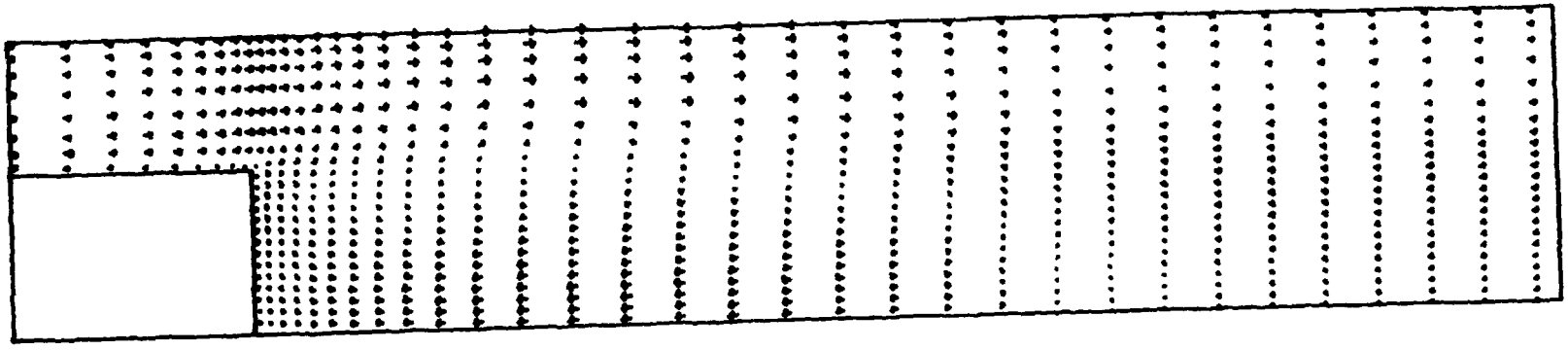

N = 80,000

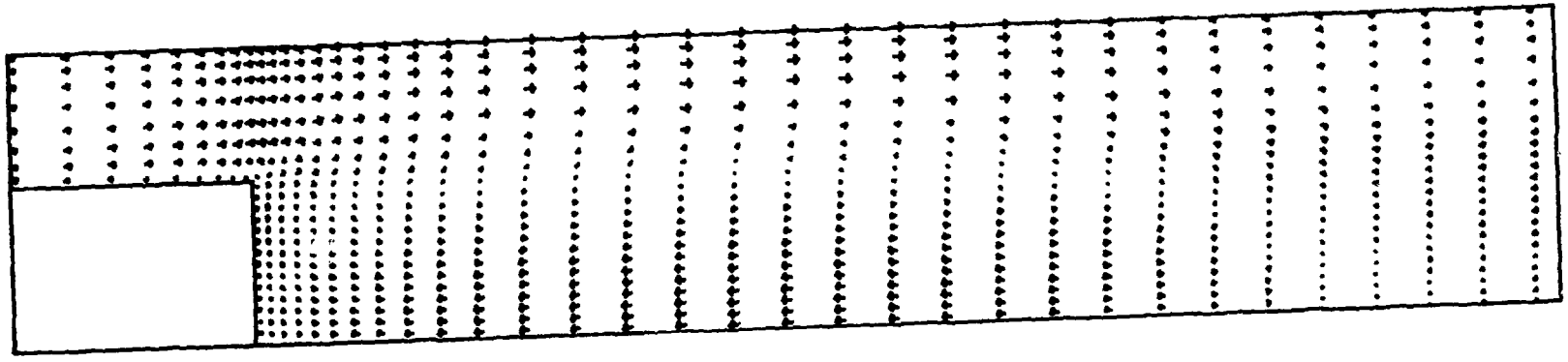

N = 90,000

Figure 4(b). Velocity-Vector Plots for Laminar-Like Calculations (Case 2) with Forcing.

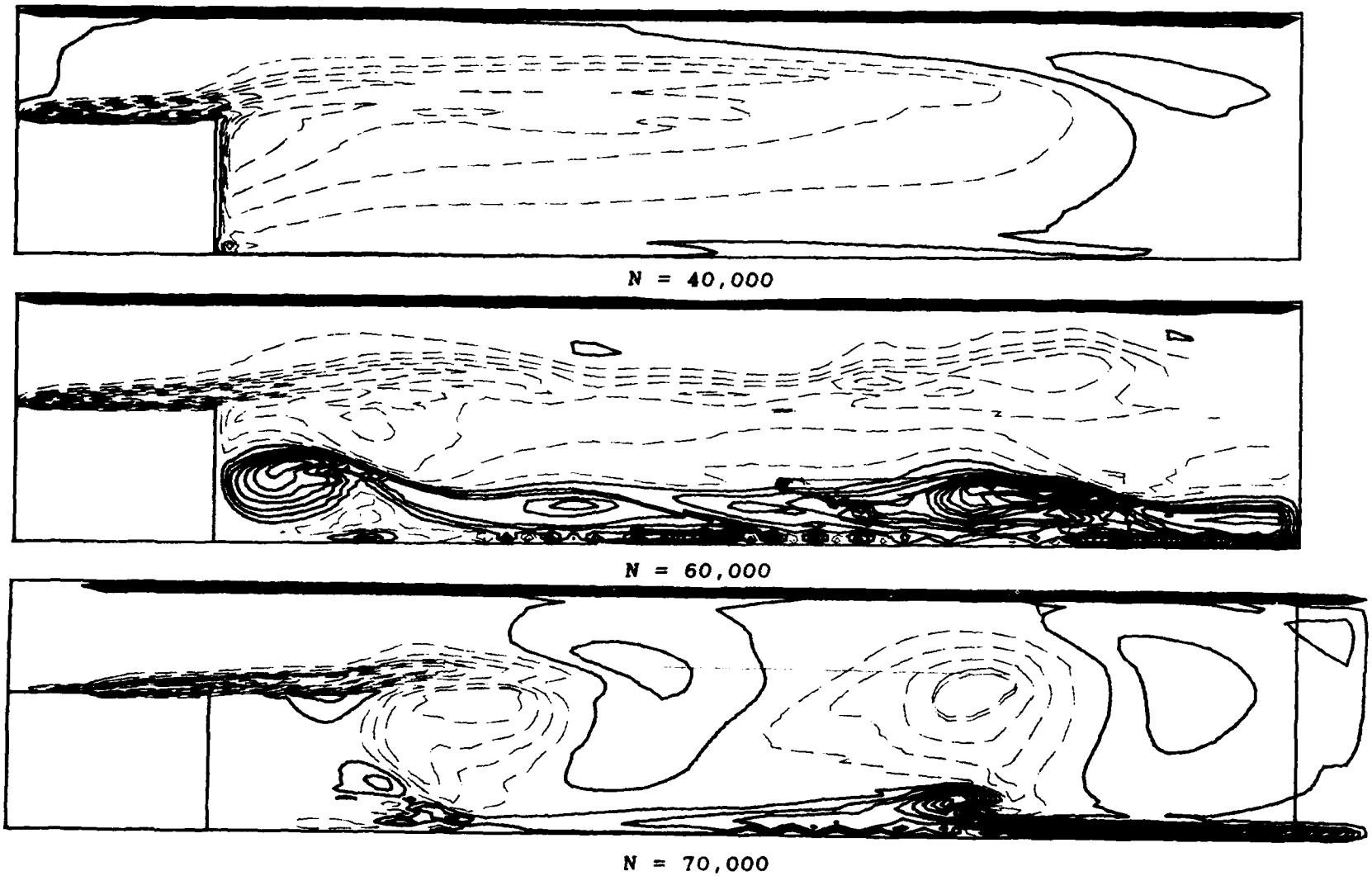

Figure 4(c). Vorticity-Contour Plots for Laminar-Like Calculations (Case 2) with Forcing.

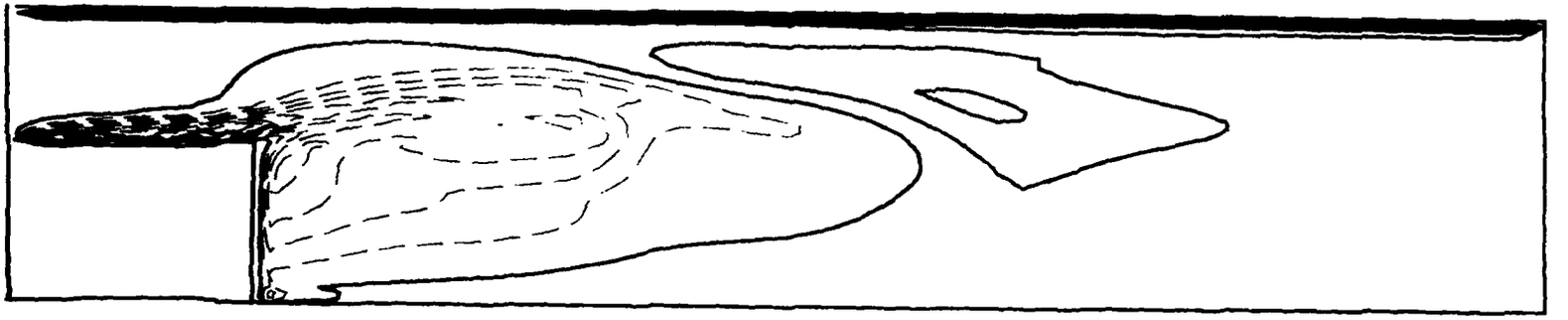

N = 80,000

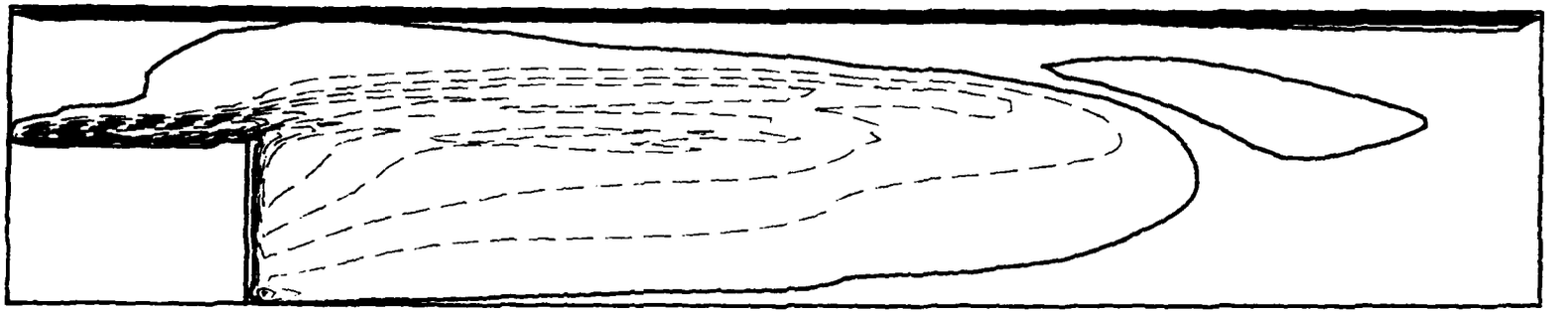

N = 90,000

Figure 4(d). Vorticity-Contour Plots for Laminar-Like Calculations (Case 2) with Forcing.

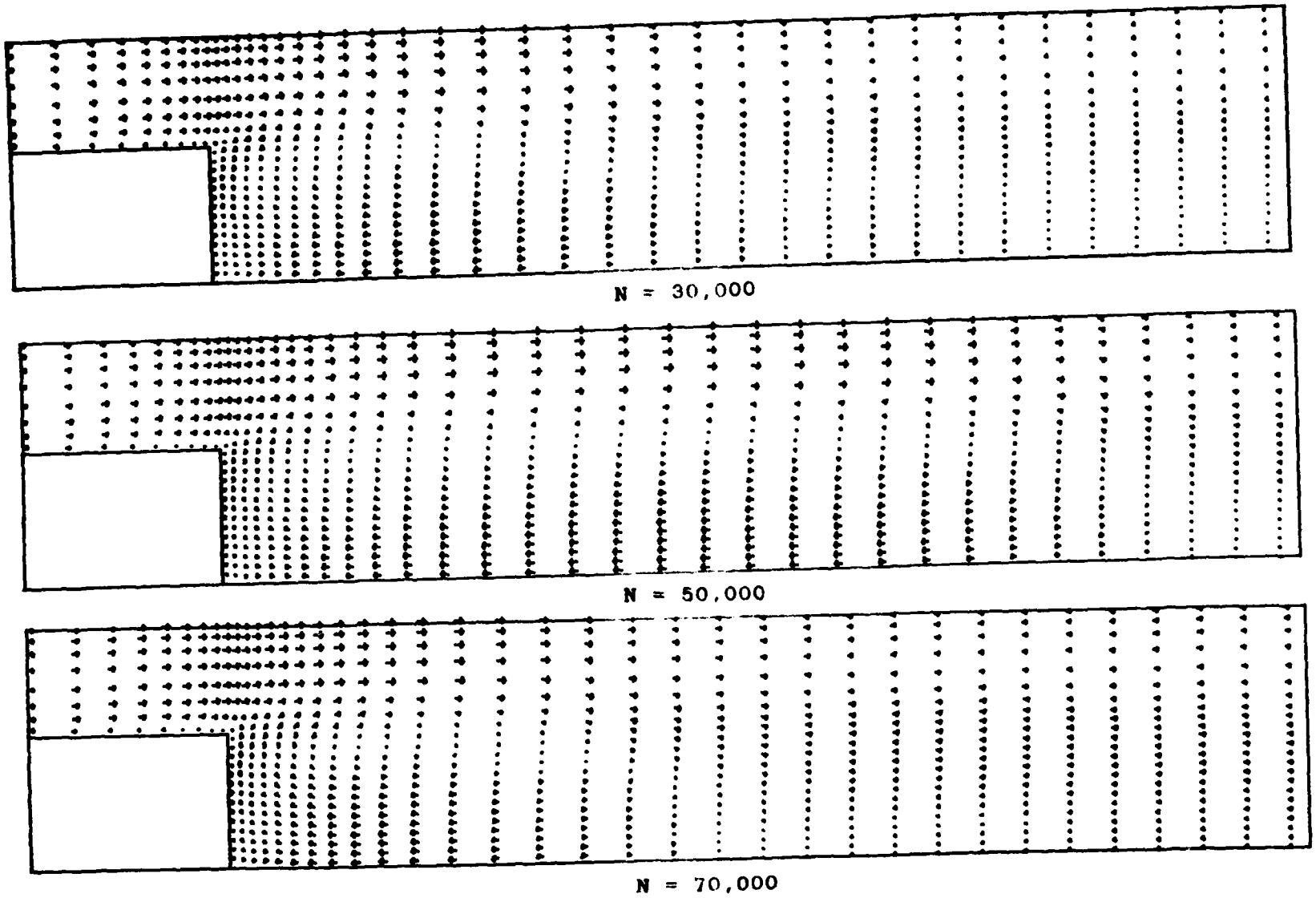

Figure 5(a). Velocity-Vector Plots for Laminar-Like Calculations (Case 3) with Forcing.

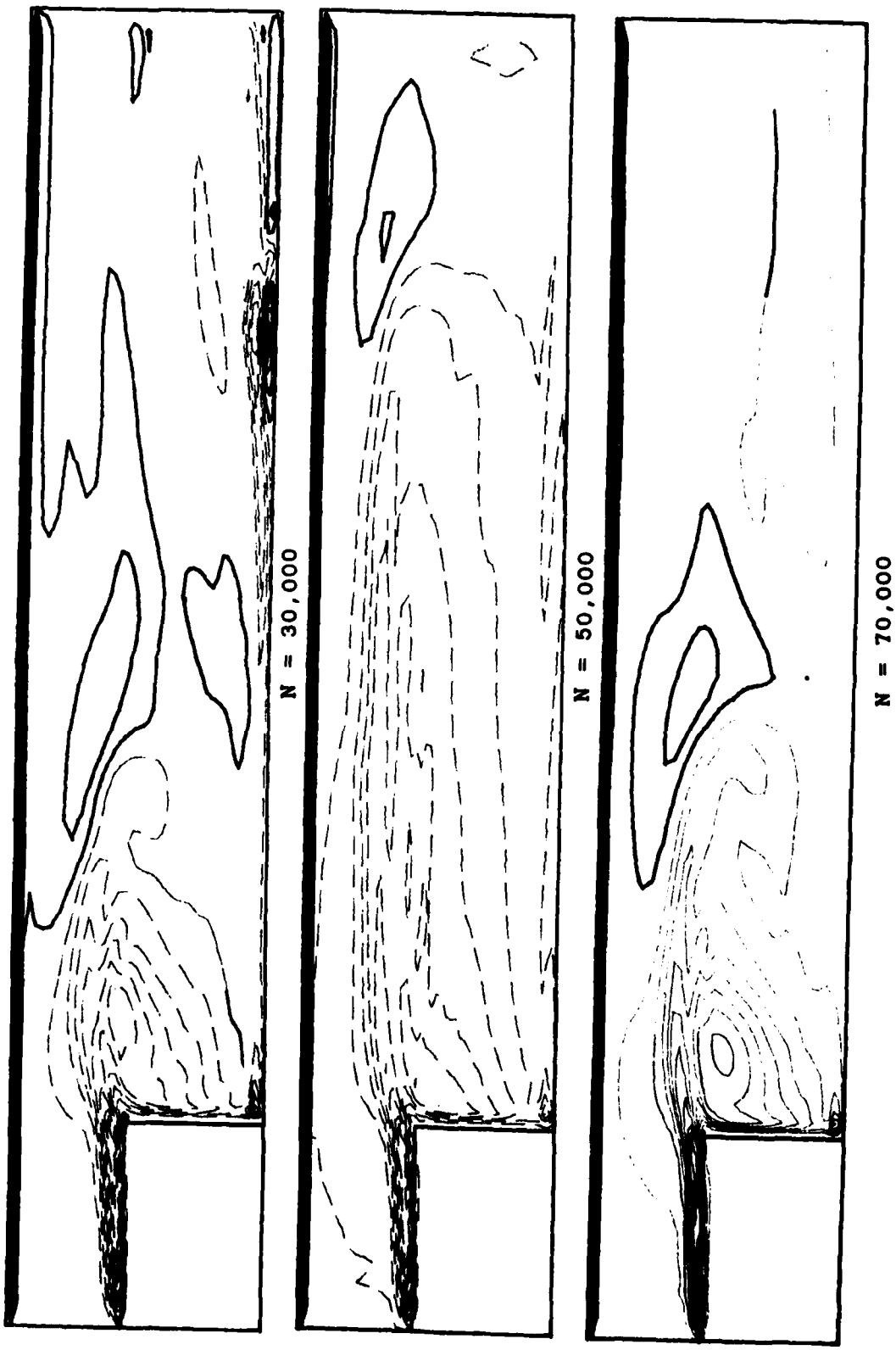

Figure 5(b). Vorticity-Contour Plots for Laminar-Like Calculations (Case 3) with Forcing.

algorithm discussed toward the end of Paragraph I.3). Thus, while the present perturbed results are not conclusive, they are further suggestive of the earlier conclusions.

b. Turbulent Flowfield Results

More definitive insights appear to be indicated by the calculations with the k-ε turbulence model. The inflow perturbation of this computation was the same as that of the second laminar case [see Paragraph II.3.a(2a)]. As in the case of the unforced turbulent calculations discussed in Paragraph III.1, the perturbed results are based on the (60 x 46) finite-difference grid.

Figure 6 shows the velocity-vector plots and vorticity-contour plots corresponding to different times of the perturbed turbulent-flow computations. While the vector plot at 60,000 time steps indicates that the recirculation vortex is pushed farther upstream (note the decrease in the axial coordinate of the vortex center) and that the reverse flow is present along the centerline for the entire extent of the combustor, at 70,000 time steps, the vortex has moved downstream (occupying a position similar to that in Figure 2b of the unperturbed flow) and the centerline rear stagnation point is again at a distance of approximately one centerbody diameter. Although detailed comparisons of the velocity fields obtained without and with forcing would be helpful in ascertaining the influence of time-dependent inflow conditions on the time-dependent turblent-flow calculations, Figure 6 does suggest that the particular case of forcing does not cause an oscillatory flowfield in the interior. Doubtless the question of insufficient perturbation amplitude alluded to in Paragraph III.2.a remains to be addressed in this context as well. Nevertheless, it does appear that a properly formulated turbulence model tends to damp out the initial transients and causes no downstream magnification of the shear-layer instability.

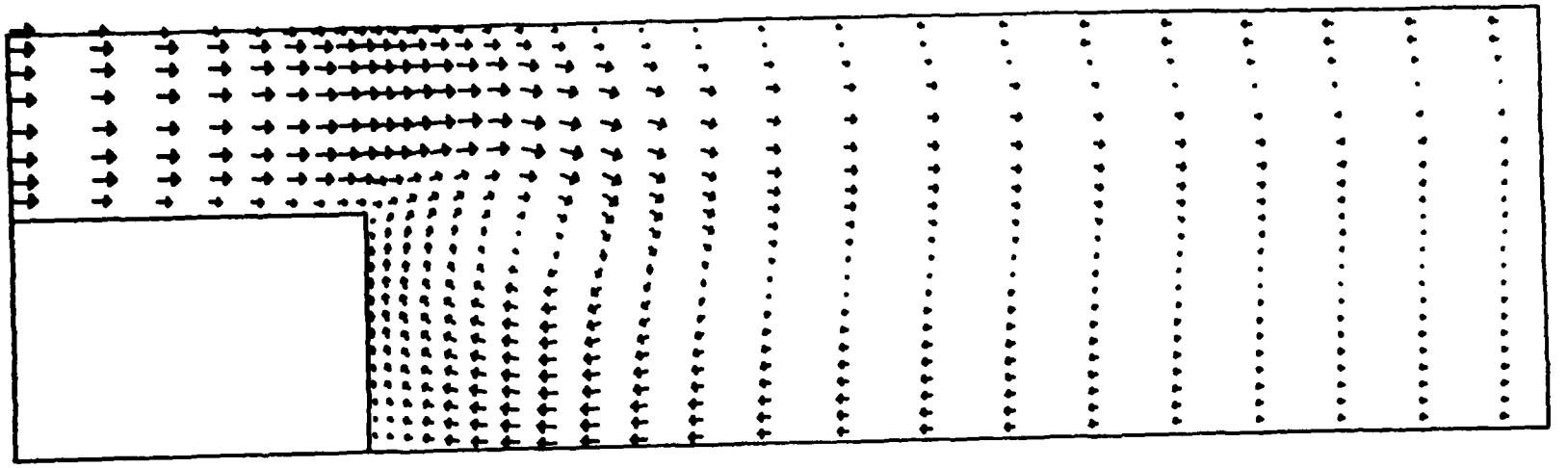

N = 60,000

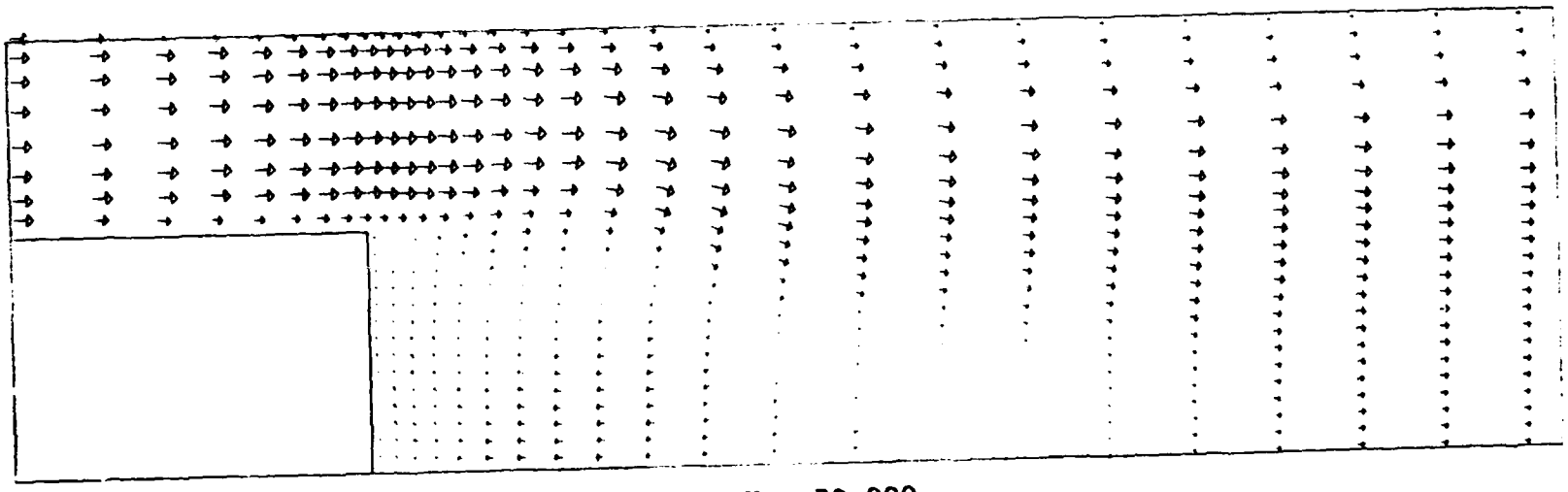

N = 70,000

Figure 6(a). Velocity-Vector Plots for Turbulent Flow with Forcing.

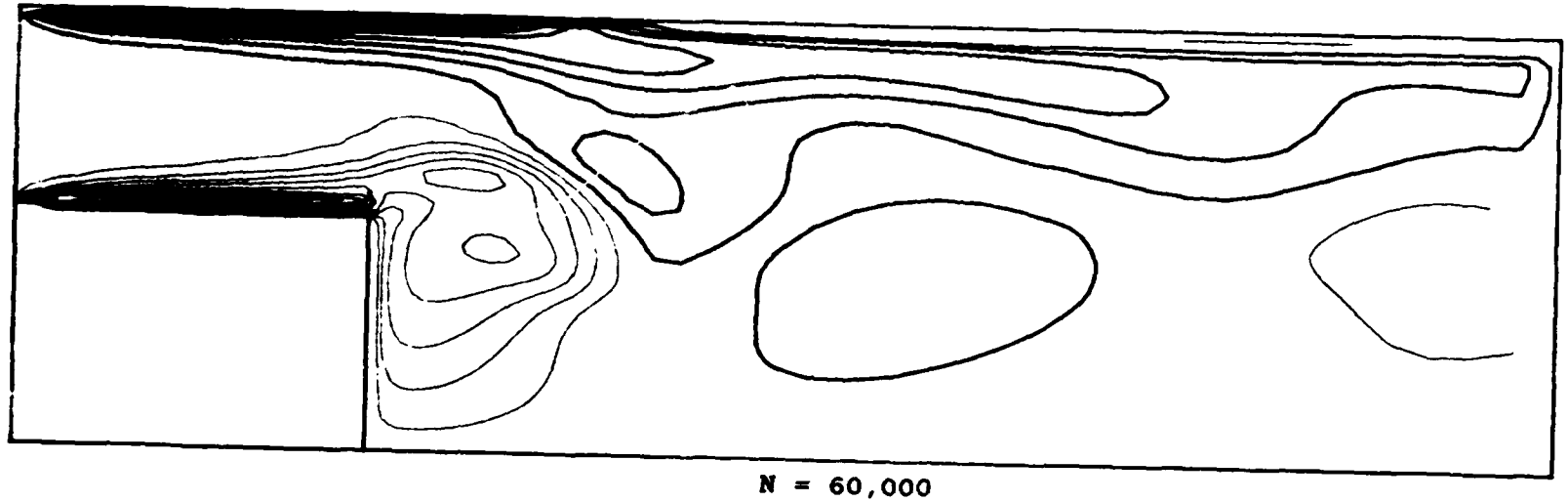

N = 60,000

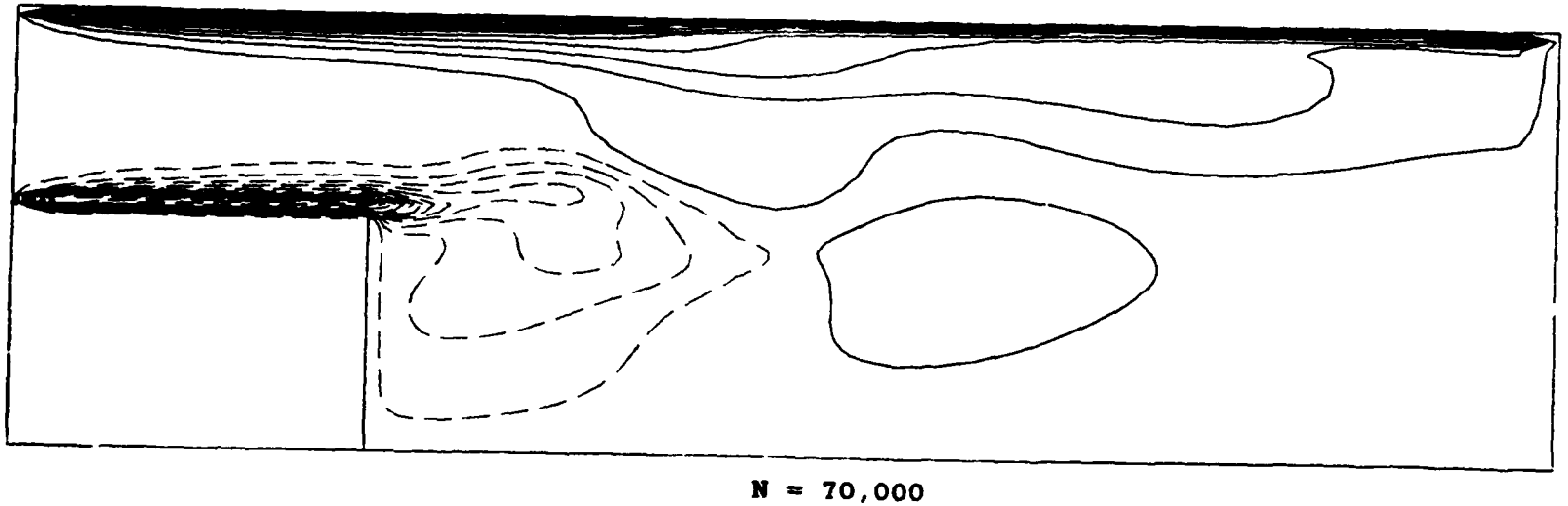

N = 70,000

Figure 6(b). Vorticity-Contour Plots for Turbulent Flow with Forcing.

SECTION IV
CONCLUSIONS AND RECOMMENDATIONS

This section summarizes the main conclusions of the assessment of time-dependent calculations for gas turbine combustor-type flows and outlines our recommendations for further computational fluid dynamic research.

1. CONCLUSIONS

The conclusions presented here stem from CFD research of limited scope addressing the nonreacting flowfield due to annular air stream in the POSF centerbody combustor. No comprehensive examination of various time-dependent computational procedures was undertaken. Attention in the present study was limited to the FIMM procedure involving the MacCormack explicit algorithm and focused on the incorporation of the k-ϵ turbulence model in the time-dependent formulation. Thus, this study represents the solution of the Reynolds-averaged Navier-Stokes equations which retain the time-dependent terms. In view of the axisymmetric formulation and the introduction of turbulence model for all scales, the present study is not a true large-eddy simulation encompassing a subgrid-scale turbulence model. The major conclusions of this study follow:

- Calculations using the time-dependent Navier-Stokes equations with a properly formulated k-ϵ turbulence model lead to a stationary recirculating vortex in the near-wake region of the centerbody for the POSF combustor.

- This asymptotic tendency to reach a steady-state solution at large times, which was suggested by our earlier laminar-like calculations, now confirms those results and clearly demonstrates that the previous unsteady feature

of a slow migration of the recirculating vortex was caused by the lack of a turbulence model in the time-dependent formulation.

- The asymptotically reached steady-state solution of the time-dependent problem exhibits a recirculating vortex which compares reasonably well with that obtained from the solution of time-averaged equations with the k-ϵ turbulence model. This agreement extends to the locations of both the vortex center and the centerline rear stagnation point.

- Calculations employing time-dependent perturbations of inflow boundary conditions for both laminar-like and turbulent flows do not show any oscillatory behavior in the interior of the POSF configuration. However, these results with time-dependent boundary conditions are neither comprehensive nor complete enough to offer definite conclusions about the capability to predict forced oscillations in the POSF combustor.

- The attainment of steady-state solutions shows that the FIMM procedure does not capture the dynamic features of the confined recirculating turbulent flowfield of the POSF combustor. This was strongly suggested previously by the laminar-like computations with different combinations of inflow and outflow boundary conditions in two different finite-difference grids and is clearly demonstrated now by the turbulent-flow computations with k-ϵ model.

- The shedding-like behavior reported by the earlier preliminary calculations is not supported by both the subsequent laminar-like computations and the present turbulent-flow calculations and must therefore be considered suspect. Indeed, this conclusion remains

tenable after a recent exchange of views,[2] published subsequent to our submission of the draft Final Report. When some of the apparent deficiencies in the preliminary calculations which led to the shedding-like behavior of numerical origin were corrected, the FIMM calculation procedure failed to predict the dynamic behavior of the POSF flowfield. We believe that it is important to address (a) the fact that the laminar-like computations with an extended domain (which obviated the incompatibility of the exit-boundary conditions) led to a stationary vortex in the near wake and (b) the corroborative results reported elsewhere for a ramjet dump combustor for which the time-dependent formulation involving the MacCormack algorithm and the algebraic mixing-length turbulence model gave rise to a steady-state solution. The key point of the present study, therefore, is to emphasize that even relatively crude turbulence models, when incorporated in a time-dependent formulation and properly computed, predict steady-state solutions asymptotically for large times and that the accounting for turbulence dissipation could well be the essential ingredient that eliminates a violent self-sustained oscillation unrealistically obtained by a laminar-like computation of high-Reynolds-number flows.

- The experimentally observed vortex shedding in combustion flows of the POSF combustor is less likely to be an example of unsteady flow caused by the instability and its amplification in the separated shear layers than one due to the coupling between combustion heat release and duct acoustics.

---

2 See Readers' Forum, AIAA Journal 24, April 1986, pp. 698-701:
M S. Raju, M. J. Creed, and L. Krishnamurthy, Comment on "Numerical Simulation of Cold Flow in an Axisymmetric Centerbody Combustor."
J. N. Scott and W. L. Hankey Jr., Reply by Authors to M. S. Raju, M. J. Creed, and L. Krishnamurthy.

2. RECOMMENDATIONS

This limited study has not addressed the evaluation of time-dependent computational schemes from the viewpoint of numerical accuracy and computational efficiency, applicability to complex turbulent flows, extension to include combustion, swirl, liquid phase and three-dimensional effects, and comparison with experimental data. Nevertheless, such a CFD examination of gas turbine combustor-type flows is worthwhile and must be encouraged. Accordingly, we reiterate and emphasize the following recommendations offered in our previous study:

- Continue with the time-averaged formulation (involving Reynolds-averaged equations in nonreacting flows and Favre-averaged equations in reacting flows), but preferably a three-dimensional one in those situations wherein large-scale unsteadiness is not significant. To properly account for anisotropic effects, however, direct solution of the equations for the Reynolds stresses must be considered.

- Consider the numerical simulation of those flows, wherein a quasiperiodic mean flow having a characteristic frequency much smaller than the characteristic frequency of the typical large eddies is encountered, by means of the Reynolds-averaged (or Favre-averaged) formulation which includes an explicit time-dependence. Initial consideration of two-dimensional (planar) and axisymmetric flows and the use of k-ϵ model could be followed by the extension to three-dimensional geometry and algebraic stress models.

- Explore numerical simulation through time-dependent, three-dimensional Navier-Stokes equations as a large-eddy simulation approach with subgrid-scale turbulence modeling in nonreacting flows that may be regarded as simpler subsets of the complex gas turbine combustor-type flows. Viable approaches should be subsequently extended to address reacting flows.

REFERENCES

1. G. M. Corcos and F. S. Sherman, "The Mixing Layer: Deterministic Models of a Turbulent Flow. Part 1. Introduction and the Two-Dimensional Flow," J. Fluid Mech. 139, 1984, pp. 29-65.

2. G. J. Sturgess, "Stationary State Computational Fluid Dynamics for Aero-Propulsion Devices," JANNAF Propulsion, Meeting, New Orleans, LA, March 1984.

3. A. Roshko, "The Plane Mixing Layer: Flow Visualization Results and Three Dimensional Effects," Lecture Notes in Physics 136, Springer-Verlag, 1981.

4. "Numerical Flowfield Modeling Studies in a Centerbody Combustor," Contract No. F33615-82-K-2252, University of Dayton Research Institute, Dayton, OH 45469.

5. W. M. Roquemore et al., "Influence of the Vortex Shedding Process on a Bluff-Body Diffusion Flame," AIAA-83-0335, January 1983.

6. J. S. Shang, JSAXIS Computer Program, AFWAL/FIMM, 1982.

7. J. N. Scott and W. L. Hankey, Jr., "Numerical Simulation of Cold Flow in an Axisymmetric Centerbody Combustor," AIAA-83-1741, July 1983; also AIAA Journal, 23, May 1985, pp. 641-649.

8. L. Krishnamurthy, M. S. Raju, M. J. Creed, and J. N. Memering, "Time-Averaged and Time-Dependent Computations of Isothermal Flowfields in a Centerbody Combustor," AFWAL-TR-84-2081, December 1984.

9. L. Krishnamurthy, S. O. Park, D. J. Wahrer, and H. S. Cochran, "Laser Diagnostic Development and Measurement and Modeling of Turbulent Flowfields of Jets and Wakes, Part II: Numerical Predictions of Isothermal Flowfields in a Ducted Centerbody Combustor," AFWAL-TR-83-2044, June 1983.

10. K. M. Case, F. J. Dyson, E. A. Frieman, C. E. Grosch, and F. W. Perkins, "Numerical Simulation of Turbulence," Stanford Research Institute, Menlo Park, CA, Report AD-774-161, Nov. 1973.

11. D. R. Chapman, "Computational Aerodynamics Development and Outlook," AIAA Journal, 17, 1979, pp. 1293-1313.

12. B. S. Baldwin and H. Lomax, "Thin Layer Approximation and Algebraic Model for Separated Flow," AIAA-1978-257, January 1978.

13. W. J. Feiereisen, W. C. Reynolds, and J. H. Ferziger, "Numerical Simulation of a Compressible, Homogeneous, Turbulent Shear Flow," NASA-CR-164953, Report TF-13, Dept. of Mechanical Engineering, Stanford University, Stanford, CA, March 1981.

14. W. P. Jones, and B. E. Launder, "The Prediction of Laminarization with a Two-Equation Model of Turbulence," Int. J. Heat Mass Transfer, 15, 1972, p. 301.

15. W. P. Jones and B. E. Launder, "The Calculation of Low-Reynolds-Number Phenomena with a Two-Equation Model of Turbulence," Int. J. Heat Mass Transfer, 16, 1973, p. 1119.

16. K. Hanjalic and B. E. launder, "Contribution Towards a Reynolds-Stress Closure for Low-Reynolds-Number Turbulence," J. Fluid Mech., 74, 1976, p. 593.

17. L. M. Chiapetta, "User's Manual for a TEACH Computer Program for the Analysis of Turbulent, Swirling, Reacting Flow in a Research Combustor," NASA Contract NAS3-22771, United Technologies Research Center Report R83-015540-27, September 1983.

18. J. P. Drummond, "Numerical Study of a Ramjet Dump Combustor Flowfield," AIAA Journal, 23, April 1985, pp. 604-611.

19. S. W. Zelazny, A. J. Baker, and W. L. Rushmore, "Modeling of Three-Dimensional Mixing and Reacting Ducted Flows," NASA CR-2661, April 1976.

20. J. N. Memering, "Computational Studies of a Bluff-Body Combustor Flowfield," University of Dayton Honors Thesis, April 1985.

21. G. J. Sturgess and S. A. Syed, "Possible Explanation of the Dynamic Behavior of Turbulent Flow in a Widely-Spaced Co-Axial Jet Diffusion Flame Combustor," AIAA-83-0575, January 1983.

22. S. Fujii and K. Eguchi, "A Comparison of Cold and Reacting Flows Around a Bluff-Body Flame Stabilizer," J. Fluids Engng., 103, 1981, pp 328-334.

23. V. P. Lyashenko and V. I. Yagodkin, "Analysis of Reacting Gas Flow Behind a Flame Stabilizer in a Plan Channel," Combustion, Explosion and Shock Waves, 19, 1984, pp. 583-587.

24. W. M. Roquemore, R. S. Tankin, H. H. Chiu, and S. A. Lottes, "The Role of Vortex-Shedding in a Bluff-Body Combustor," ASME Winter Annual Meeting, New Orleans, Louisiana, Dec. 1984.

U.S.Government Printing Office: 1986 — 646-067/40907


FILMED
08